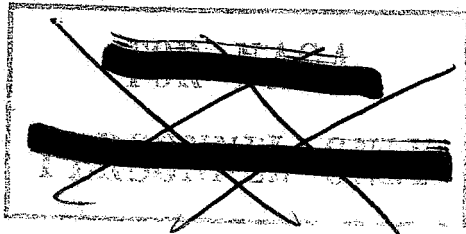NASA Project Apollo Working Paper No. 1044

PROJECT APOLLO

EFFECTS OF A NUMBER OF MODIFICATIONS

ON THE STATIC STABILITY

OF THE APOLLO ATMOSPHERIC ABORT CONFIGURATION

DISTRIBUTION AND REFERENCING

This paper is not suitable for general distribution or referencing. It may be referenced only in other working correspondence and documents on Project Apollo by participating organizations.

NATIONAL AERONAUTICS AND SPACE ADMINISTRATION
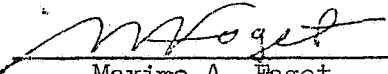
MANNED SPACECRAFT CENTER

Houston, Texas

February 28, 1962

NASA PROJECT APOLLO WORKING PAPER NO. 1044

PROJECT APOLLO

EFFECTS OF A NUMBER OF MODIFICATIONS

ON THE STATIC STABILITY

OF THE APOLLO ATMOSPHERIC ABORT CONFIGURATION

_____
Robert H. Moore, Jr.
Engineering Technician (General)

Authorized For Distribution:

_____
Maxime A. Faget
Assistant Director for
Research and Development

NATIONAL AERONAUTICS AND SPACE ADMINISTRATION

MANNED SPACECRAFT CENTER

Houston, Texas

February 28, 1962

TABLE OF CONTENTS

ii

LIST OF TABLES

LIST OF FIGURES

iv

LIST OF FIGURES

EFFECTS OF A NUMBER OF MODIFICATIONS ON THE STATIC STABILITY

OF THE APOLLO ATMOSPHERIC ABORT CONFIGURATION

SUMMARY

A preliminary investigation at Mach numbers from 0.5 to 1.20 has been conducted in the NASA Langley Research Center 8-foot transonic pressure tunnel on the atmospheric abort configuration with several devices mounted on the rocket case and the abort tower. These devices consist of two different diameter turning vanes mounted at the base of the rocket case, two different diameter blunt-cone shields mounted at the spacecraft nose within the abort tower and a blunt-cone shield mounted within the tower near the tower midpoint. Also, an investigation at Mach numbers of 1.57, 1.80, and 2.16 has been conducted in the Langley Unitary Plan wind tunnel on an atmospheric abort configuration with a flow deceleration ring device mounted on the abort tower and a redesigned solid abort tower configuration. These tests were run with and without a conical shroud around the abort rocket nozzles.

The transonic data for the configuration with the several devices show that all of the configurations are fairly stable throughout the Mach number range and are very similar. The configuration with the large blunt-cone shield mounted at the spacecraft nose within the abort tower was the only modification which improved the stability of the reference configuration. However, the improvement was noted at higher angles of attack and the reference configuration still exhibited the best low angle-of-attack stability.

The supersonic data for the solid abort tower configuration and the basic atmospheric abort configuration with the flow deceleration ring device show the configurations to be stable throughout the Mach number range tested with and without the conical shroud around the abort rocket nozzles. The addition of the conical shroud to the solid tower configuration increased the static stability at the lower angles of attack and decreased the static stability at the higher angles of attack over the supersonic Mach number range tested. The data for the basic atmospheric abort configuration with the flow deceleration ring device show that the addition of the conical shroud tends to decrease the static stability. No improvement in stability characteristics of the basic configuration was observed over the angle-of-attack range tested due to the modification made.

The data from all of the configurations and devices tested show no improvement in the stability characteristics over the original abort configuration near Mach number 1.00 where the stability is critical.

INTRODUCTION

The results of tests on a representative Apollo atmospheric abort configuration, reported in reference 1, indicated a lack of stability near a Mach number of 1.00, and also a discontinuity of low angles of attack in the pitching-moment data near $M = 1.57$. Unpublished results of tests made in the Langley Unitary Plan wind tunnel on the C-1 Saturn Apollo launch configuration indicated that a conical shroud or fairing around the abort rocket nozzles eliminated the discontinuity in the moment data near $M = 1.57$. Tests were conducted in the Langley 8-foot transonic pressure tunnel and the Langley Unitary Plan wind tunnel with and without a conical shroud around the abort rocket nozzles on a modified atmospheric abort configuration. Two modifications were made to the basic abort configuration reported in reference 1. The rocket fineness ratio was increased in an attempt to increase the stability characteristics of the configuration, and the afterbody angle was decreased from 35° to 33° in order to obtain more workable volume in the command module. The data for these tests are reported in reference 2. The basic moment data reported in reference 2 are presented for five center-of-gravity locations, four of which are not on the axis of symmetry. The result of the data reported in reference 2 indicated that the configuration without the conical shroud had satisfactory stability characteristics for the most forward moment center only. A large amount of ballast would be required at the rocket nose to obtain this center-of-gravity location. The data for this configuration are generally similar to the data reported in reference 1. It was concluded that since the data are similar, any improvement in stability due to the increase of the rocket fineness ratio was counteracted by a decrease in stability due to the change in the afterbody angle. The configuration with the conical shroud reported in reference 2 indicated the addition of the conical shroud provides a margin of positive stability for all moment centers. Also, the addition of the conical shroud tends to eliminate or lessen the discontinuity in the moment data near $M = 1.57$.

In an attempt to improve the stability characteristics of the shrouded configuration reported in reference 2, a series of modifications were investigated. A completely redesigned solid tower for the abort configuration and several devices added to the basic abort configuration reported in reference 2 were tested. The solid tower configuration was based on the minimum size solid tower that could be obtained from a static structural load standpoint.

Tests were conducted in the Langley 8-foot transonic pressure tunnel on the basic abort configuration of reference 2 with several devices mounted on the tower and on the rocket case. These devices consist of two different diameter flow turning vanes located at the base of the rocket case, two different diameter blunt-cone shields attached at the

base of the abort tower at the spacecraft nose, and a blunt-cone shield located within the escape tower near the tower midpoint. The tests were conducted at Mach numbers from 0.5 to 1.20 at angles of attack from about -2° to 20°. These tests were run without the conical shroud around the abort rocket nozzles. Tests were conducted in the Langley Unitary Plan wind tunnel on the solid tower configuration and the basic abort configuration of reference 2 with a flow deceleration ring device at Mach numbers of 1.57, 1.80, and 2.16 and at angles of attack from about -10° to 20°. These tests were run with and without the conical shroud around the abort rocket nozzles. The purpose of this paper is to report the results of these tests.

SYMBOLS

Data are presented using both the body and stability systems of axes. The stability system of axes is shown in figure 1. The symbols and coefficients used in this paper are defined as follows:

C_m pitching-moment coefficient, $\dfrac{\text{Pitching moment}}{qSD}$

D reference dimension (maximum model diameter), ft

M free-stream Mach number

P free-stream static pressure, lb/sq ft

q free-stream dynamic pressure, $0.7PM^2$, lb/sq ft

R Reynolds number based on maximum diameter

S reference area, $\frac{\pi}{4}D^2$, sq ft

$\dfrac{X}{D}$ longitudinal location of the center of gravity from heat shield face

$\dfrac{Z}{D}$ vertical location of the center of gravity

α angle of attack of model center line, deg

c.g.   center-of-gravity location

MODELS

General dimensions of the configurations tested are given in figure 2, and photographs of the configurations mounted in the test facilities are given in figure 3. The test models were made of stainless steel and aluminum. The spacecraft had a maximum diameter, D = 10.92 inches, the heat shield radius is 1.2D, and the corner radius is 0.05D. The after-body angle is 33°.

The basic atmospheric abort configuration is the same as the basic configuration of reference 2. The solid tower atmospheric abort configuration was designed with a minimum size solid tower that could be obtained from a static structural load standpoint.

TEST FACILITIES, RANGES, AND ACCURACIES

The tests were conducted in the Langley 8-foot transonic pressure tunnel at Mach number range from 0.5 to 1.20 and in the Langley Unitary Plan wind tunnel at Mach numbers of 1.57, 1.80, and 2.16.

The basic atmospheric abort configuration tests with several different devices mounted on the rocket case and within the abort tower were conducted in the Langley 8-foot transonic pressure tunnel at Mach numbers from 0.5 to 1.20. These devices consist of two different diameter turning vanes mounted at the base of the rocket case, two different diameter blunt-cone shields mounted at the spacecraft nose near the tower base, and a blunt-cone shield mounted within the tower near the tower midpoint.

The basic abort configuration with the flow deceleration ring device and the solid abort tower configuration tests were conducted in the Langley Unitary Plan wind tunnel at Mach numbers of 1.57, 1.80, and 2.16.

Table I presents the test conditions for the configuration tested. Table II gives the accuracy range of the data obtained from these tests.

PRESENTATION OF RESULTS

These tests were conducted in an attempt to see if the several modifications to the atmospheric abort configuration would improve the stability characteristics over the original abort configurations. The normal force cofficient versus angle of attack curve for the configuration tested is very similar to normal force cofficient versus angle of attack

curve for the configuration reported in reference 2, thus only the pitching-moment coefficients need to be presented in this paper as these tests are oriented towards improving the static stability of the configuration.

The basic moment data for the transonic data are presented in figures 4(a) to 4(f), and the basic supersonic data are presented in figures 5(a) to 5(c). The basic moment data for all configurations have been calculated for a moment center of X/D = 0.706, Z/D = -0.0407 and is compared with data reported in reference 2 on the configuration with the conical shroud around the abort rocket nozzles at a moment center of X/D = 0.706, Z/D = -0.0407.

DISCUSSION

The longitudinal static stability data presented in this paper are the results of a brief investigation of the basic atmospheric abort configuration with several devices mounted on the rocket case and the abort tower. The basic atmospheric abort configuration was tested, with and without the conical shroud, with a flow deceleration ring device, and a redesigned solid abort tower configuration with and without the conical shroud through the Mach number range of 0.5 to 2.16. The basic moment data are presented in figures 4 and 5 and have been calculated about a moment center (X/D = 0.706, Z/D = -0.0407). The data are compared with the configuration with the conical shroud around the abort rocket nozzles reported in reference 2.

Basic Abort Configuration with Several Devices

Mounted on the Rocket Case and Abort Tower

The basic moment data for the basic abort configuration with several devices mounted on the rocket case and the abort tower were obtained from the Langley 8-foot transonic pressure tunnel at Mach number range from 0.5 to 1.20. The angles of attack investigated were from about -2° to 20°. The several devices tested consist of two different diameter turning vanes located at the base of the rocket case, two different diameter blunt-cone shields located at the spacecraft nose near the tower base, and a blunt-cone shield located within the abort tower near the tower midpoint. The basic moment data are presented in figures 4(a) to 4(f).

The data show that all of the configurations are stable throughout the Mach number range and over a fairly large angle-of-attack range. The configurations with the two different diameter turning vanes mounted at the rocket base, the small blunt-cone shield mounted at the spacecraft

nose near the tower base, and the blunt-cone shield mounted near the tower midpoint are very similar throughout the Mach number range. The configuration with the large blunt-cone shield mounted at the spacecraft nose near the tower base proved to be the most stable throughout the Mach number range and over a large angle-of-attack range. The data for the configuration with the large blunt-cone shield also show a slight increase in stability at angles of attack from 5° to 20° over the configuration reported in reference 2 except for the data at $M = 1.20$.

Supersonic data were obtained from the Langley Unitary Plan wind tunnel at Mach numbers of 1.57, 1.80, and 2.16 for the solid abort tower configuration and the basic abort configuration with the flow deceleration ring device. The angles of attack investigated were from about -10° to 18°. These tests were conducted with and without the conical shroud around the abort rocket nozzles. The basic moment data are presented in figures 5(a) to 5(c) and are compared with the configuration with the conical shroud reported in reference 2.

Solid Abort Tower Configuration

The data presented in figures 5(a) to 5(c) show that the configuration without the conical shroud around the abort rocket nozzles is stable over the Mach number range ($M = 1.57$, 1.80, and 2.16), with trim angle of about 4°. Figures 5(a) and 5(b) show that the addition of the conical shroud gives a large increase in the static stability at the low angles of attack, but at the higher angles of attack (α = about 9°) there is a large decrease in the stability. The data at the higher Mach number ($M = 2.16$) in figure 5(c) show that the addition of the conical shroud tends to decrease the stability characteristics of the configuration at all angles of attack tested.

Basic Atmospheric Abort Configuration with Flow

Deceleration Ring Device

Figures 5(a) to 5(c) show the configuration (with and without the conical shroud) with the flow deceleration ring device to be stable throughout the Mach number range. The data presented in figure 5(a) show that the configuration with and without the conical shroud is very similar and stable over a fairly large angle-of-attack range. Figures 5(b) and 5(c) show that the configuration without the conical shroud is more stable than the configuration with the conical shroud at the lower angles of attack with a decrease in stability at the higher angles of attack ($\alpha > 11^\circ$). The data presented in figure 5(c) ($M = 2.16$) show that the configuration without the conical shroud is very similar to the configuration reported in reference 2; however, the

configuration reported in reference 2 still shows the best stability characteristics throughout the Mach number range tested.

CONCLUSIONS

The results of a brief investigation of the atmospheric abort configuration with several devices mounted on the rocket case and within the abort tower, a solid abort tower configuration, and a basic abort configuration with a flow deceleration ring device indicate that there is no increase in the stability characteristics over the basic open tower shrouded nozzle configuration at the critical Mach number (M = 1.00).

REFERENCES

1. Jackson, Bruce G., and Moseley, William C., Jr.: Project Apollo - Static Longitudinal Stability Characteristics of a Blunt Symmetrical Reentry Configuration and a Tower-Mounted-Rocket Atmospheric Abort Configuration Which Meet the Apollo Mission Requirements. NASA Project Apollo Working Paper No. 1022, Jul. 19, 1961.

2. Moore, Robert H., Jr.: Project Apollo - Static Longitudinal Stability Characteristics of a Modified Atmospheric Abort Configuration for Project Apollo. NASA Project Apollo Working Paper No. 1040, Dec. 20, 1961.

TABLE I.- TEST CONDITIONS

Facility	Mach number	Stagnation pressure lb/sq in. abs	Dynamic pressure lb/sq ft	Stagnation temperature	Reynolds number[1]
Langley 8-foot transonic pressure tunnel	0.5	14.7	311	121	2.50×10^6
	.7	14.7	521	121	3.17
	.8	14.7	619	121	3.44
	.9	14.7	706	121	3.60
	1.00	14.7	783	121	3.75
	1.20	14.7	882	121	3.85
Langley Unitary Plan wind tunnel	1.57	7.0	427	125	1.89×10^6
	1.80	8.0	453	125	1.99
	2.16	10.0	468	125	2.14

[1]Based on spacecraft diameter

TABLE II.- ACCURACY OF DATA

| Facility	Mach number	Accuracy of —						
		M	α, deg	C_m	C_N	C_A	C_L	C_D
Langley 8-foot transonic pressure tunnel	0.5	±0.005	±0.2	±0.003	±0.017	±0.017	±0.017	±0.017
	.7	±.005	±.2	±.002	±.010	±.010	±.010	±.010
	.8	±.005	±.2	±.002	±.009	±.009	±.009	±.009
	.9	±.005	±.2	±.001	±.008	±.008	±.008	±.008
	1.00	±.005	±.2	±.001	±.007	±.007	±.007	±.007
	1.20	±.005	±.2	±.001	±.006	±.006	±.006	±.006
Langley Unitary Plan wind tunnel	1.57	±0.015	±0.1	±0.00049	±0.0054	±0.0054	±0.0054	±0.0054
	1.80	±.015	±.1	±.0049	±.0054	±.0054	±.0054	±.0054
	2.16	±.015	±.1	±.0045	±.0049	±.0049	±.0049	±.0049
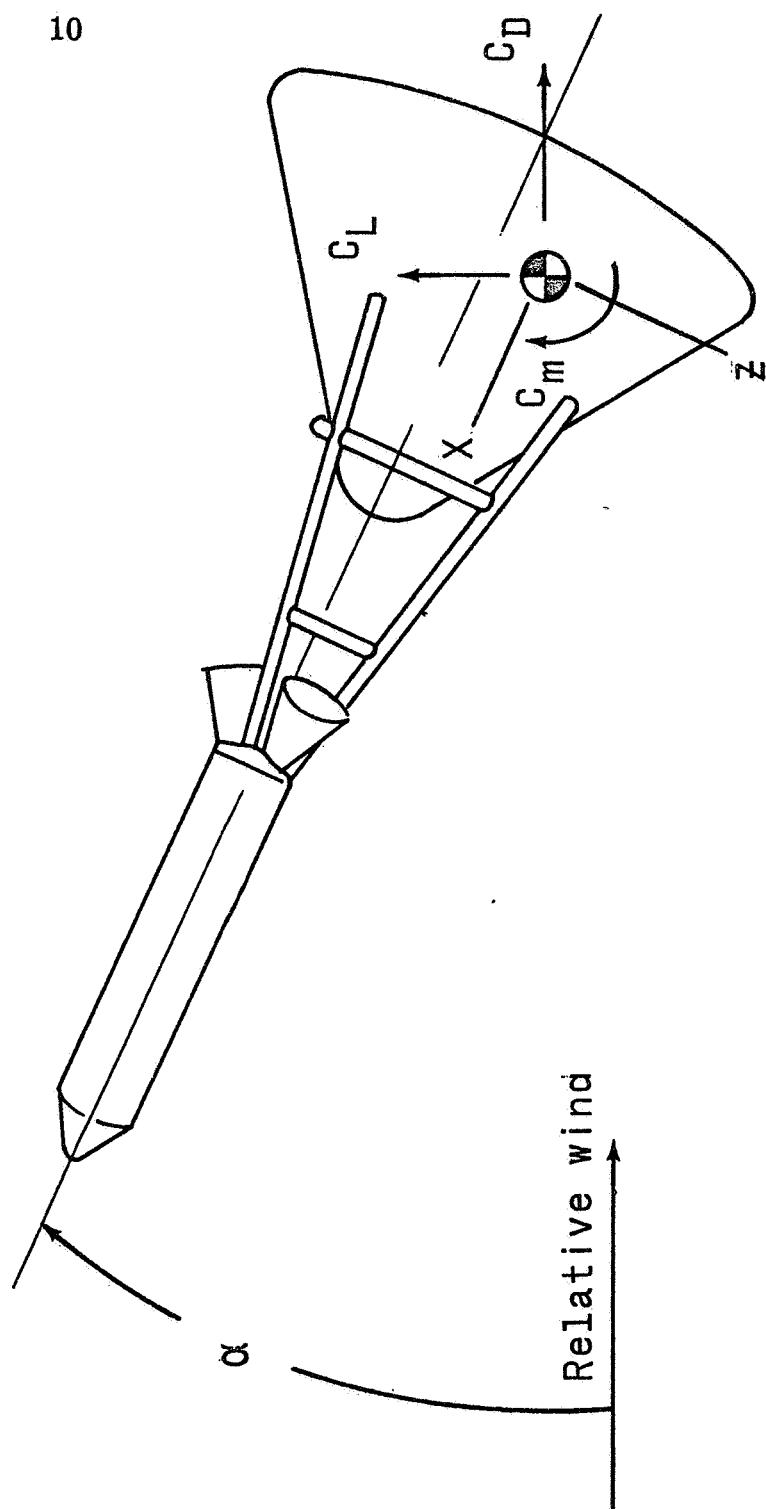
Figure 1.- Sketch showing stability axes system used.

Figure 2a.- Abort configuration with two different diameter turning vanes mounted at the base of the rocket case.
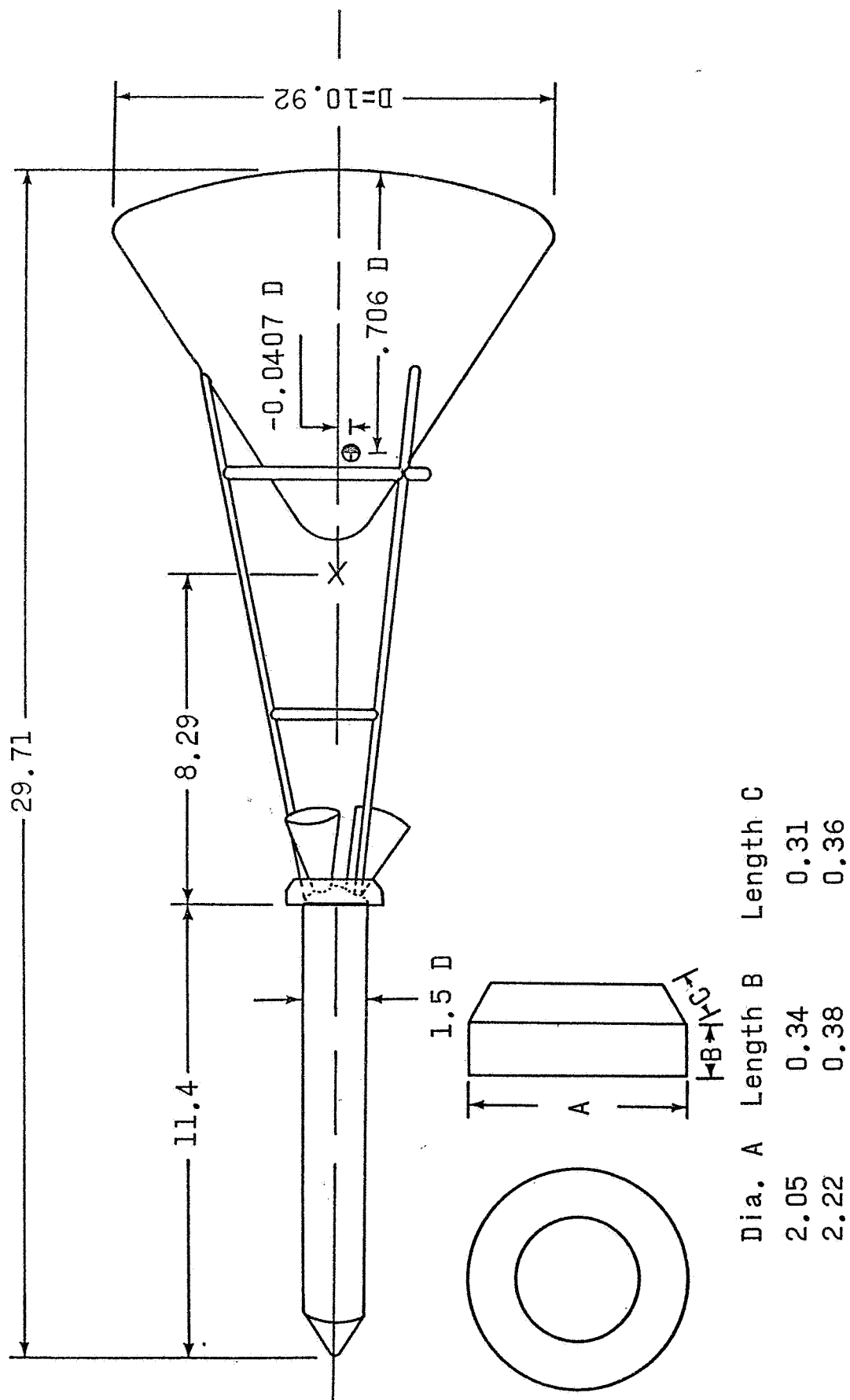
Sketch of turning vanes showing several dimensions.

Dia. A	Length B	Length C
2.05	0.34	0.31
2.22	0.38	0.36

D=10.92

29.71

8.29

11.4

1.5 D

.706 D

-0.0407 D

X

A

B C
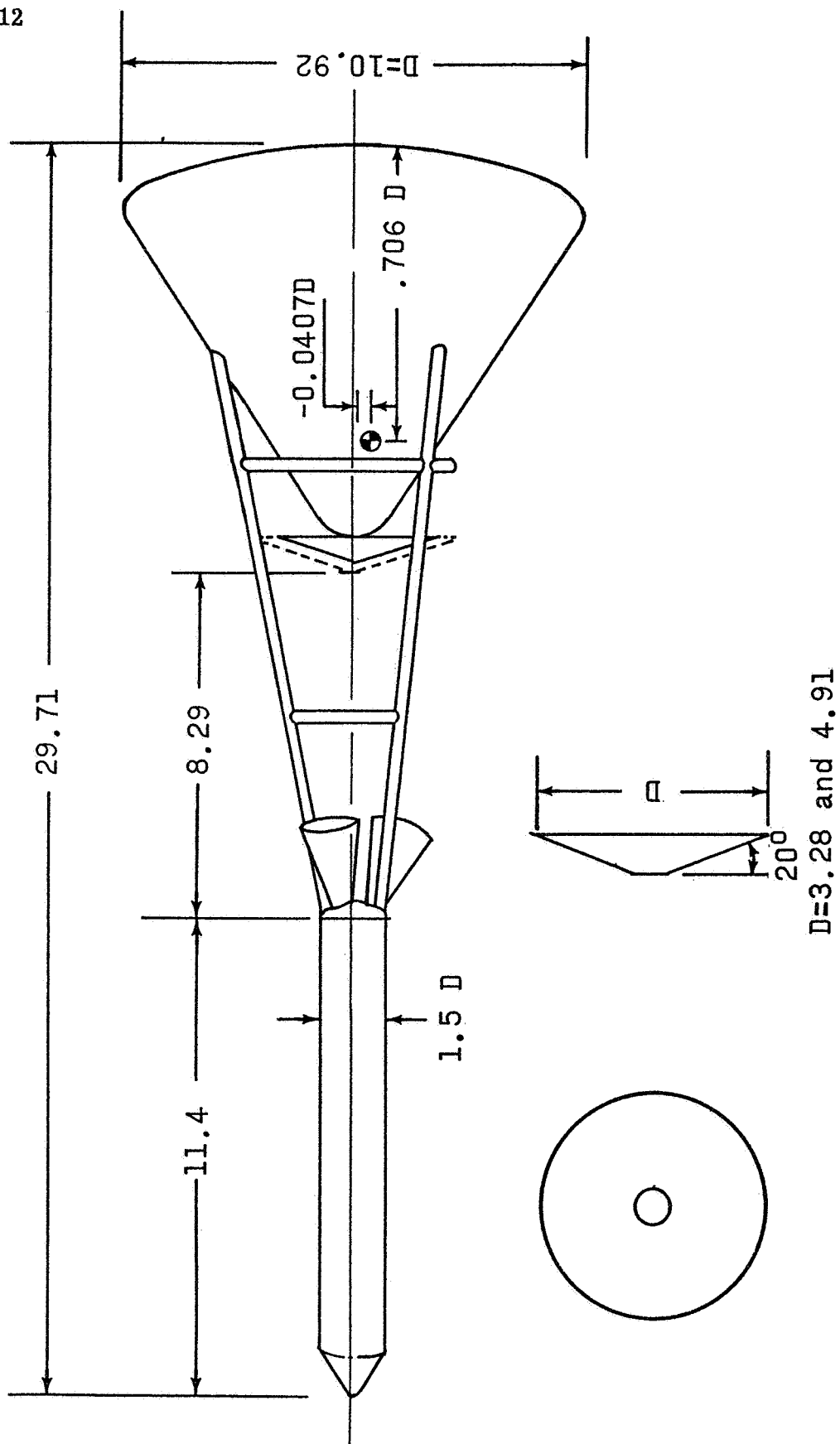
Sketch of blunt-cone showing
general dimensions.

Figure 2b. - Abort configuration with two different diameter blunt-cone
shields mounted at the spacecraft nose.

D=10.92

-0.0407 D

.706 D

2.26

29.71

8.29

11.4

3.28

20°
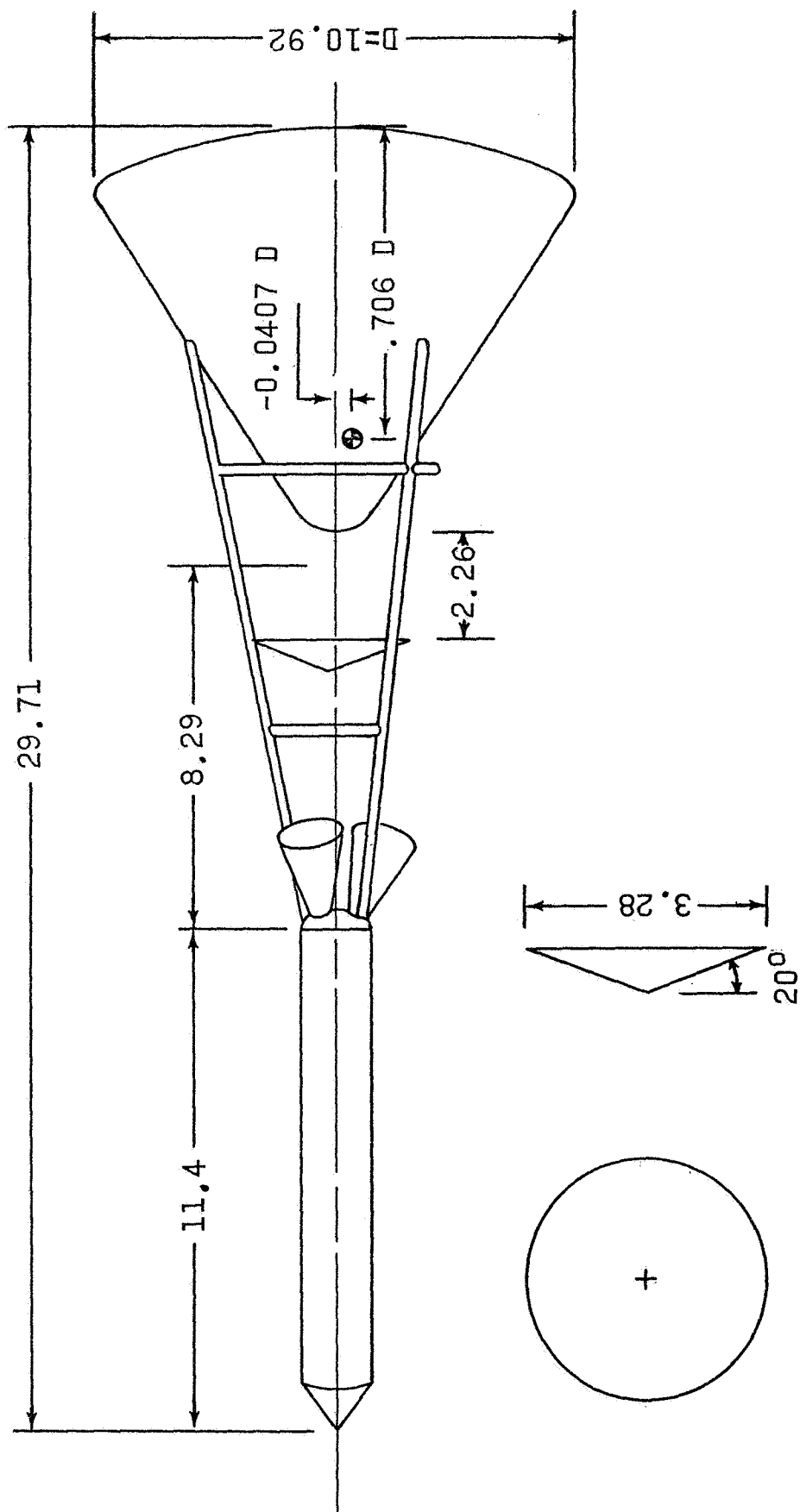
Sketch of blunt-cone shield
showing the general dimensions.

Figure 2c.- Abort configuration with blunt-cone shield near
tower midpoint.

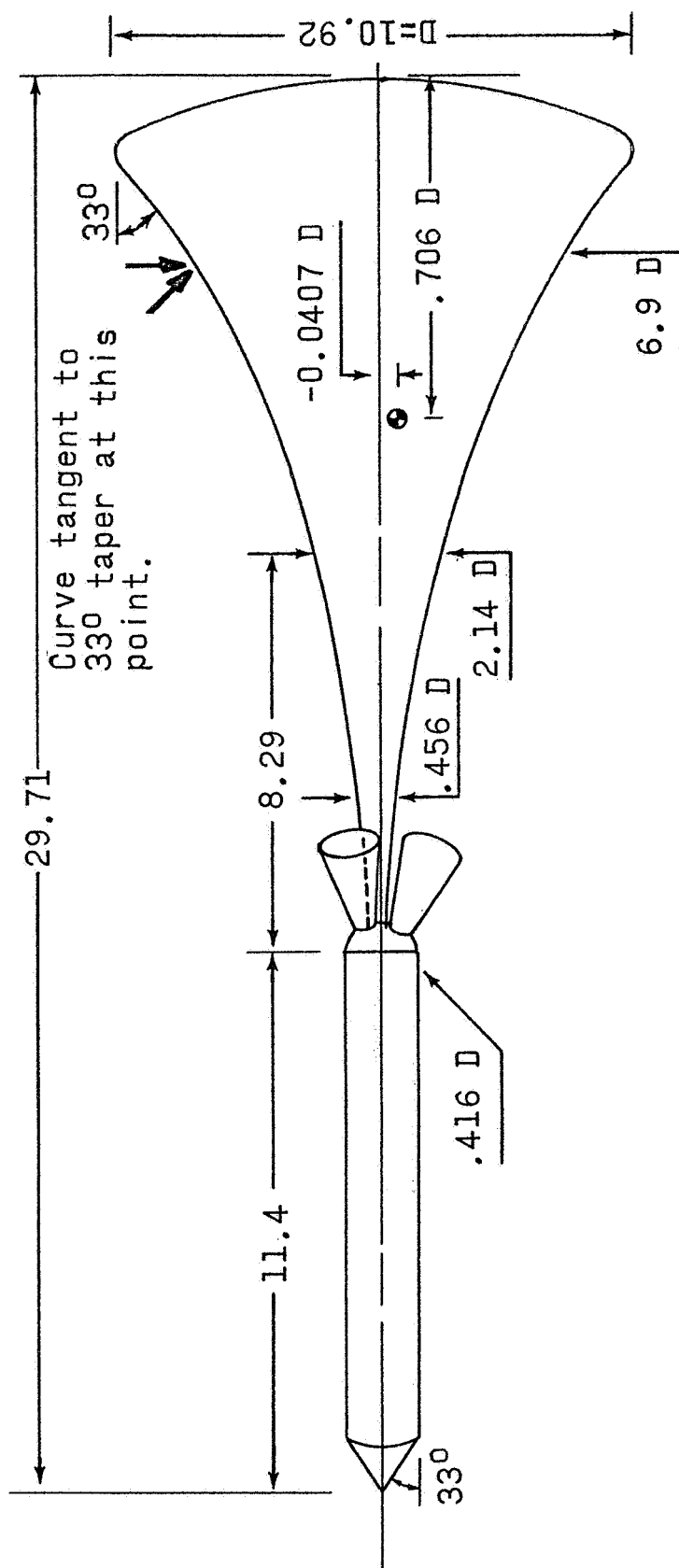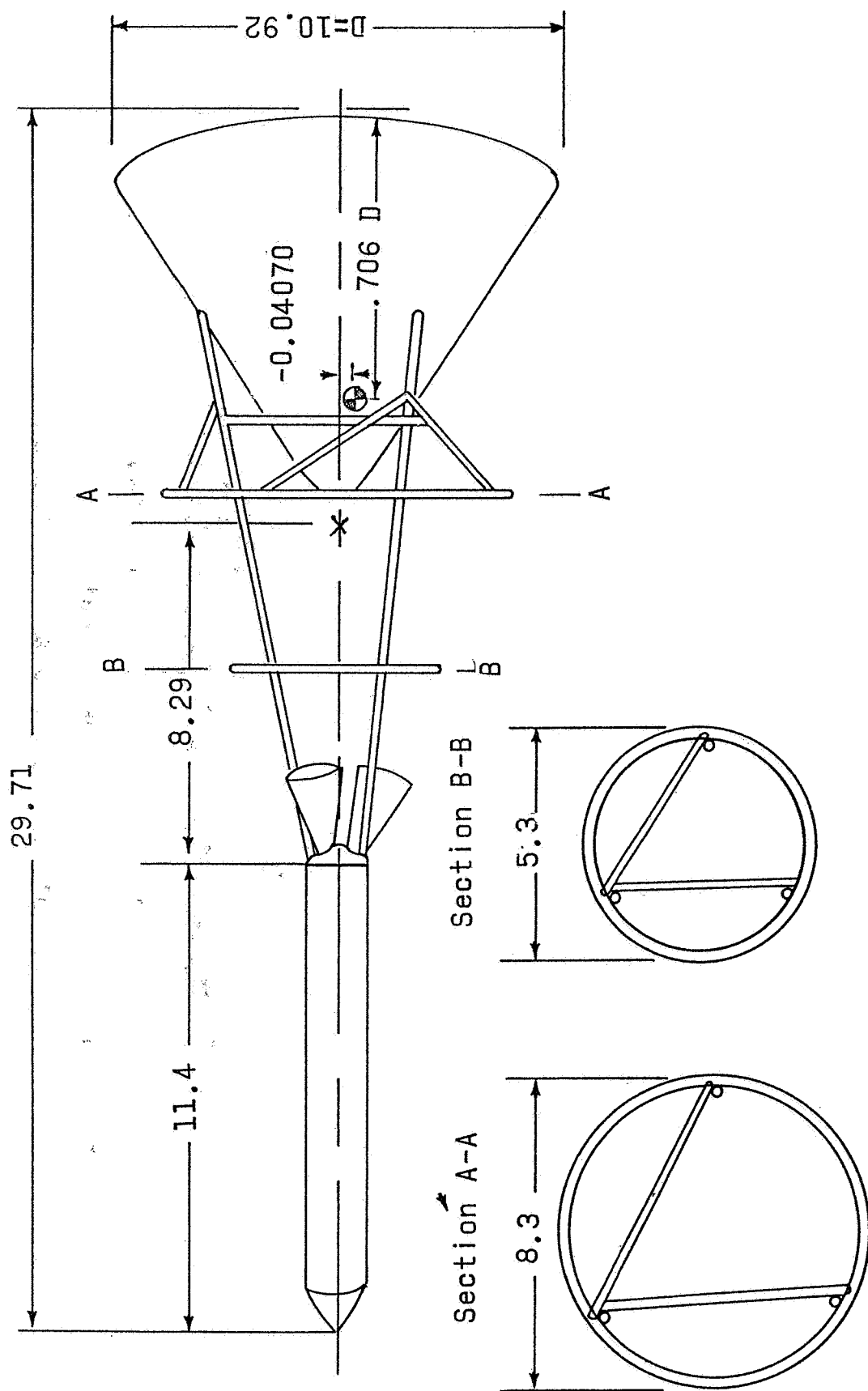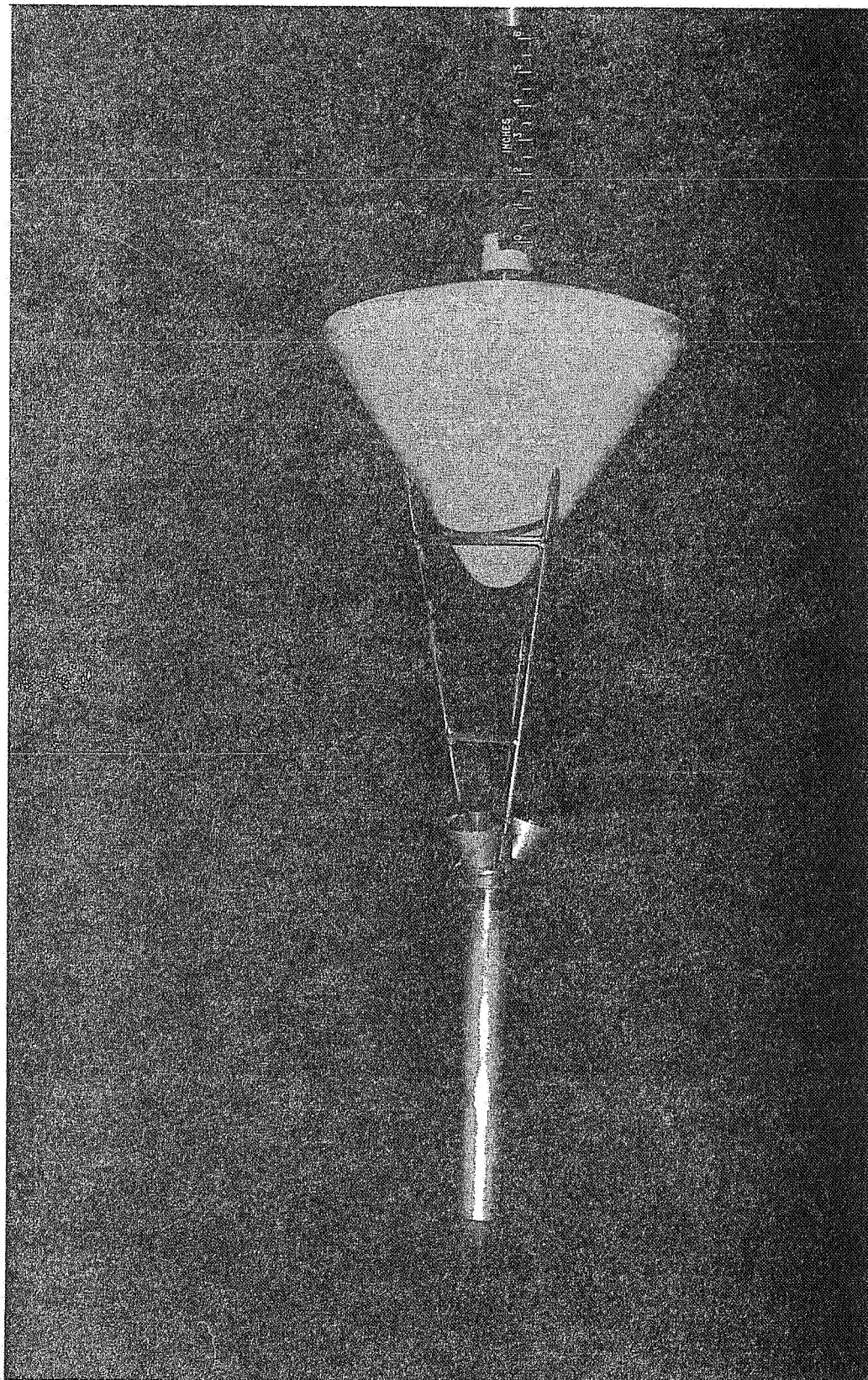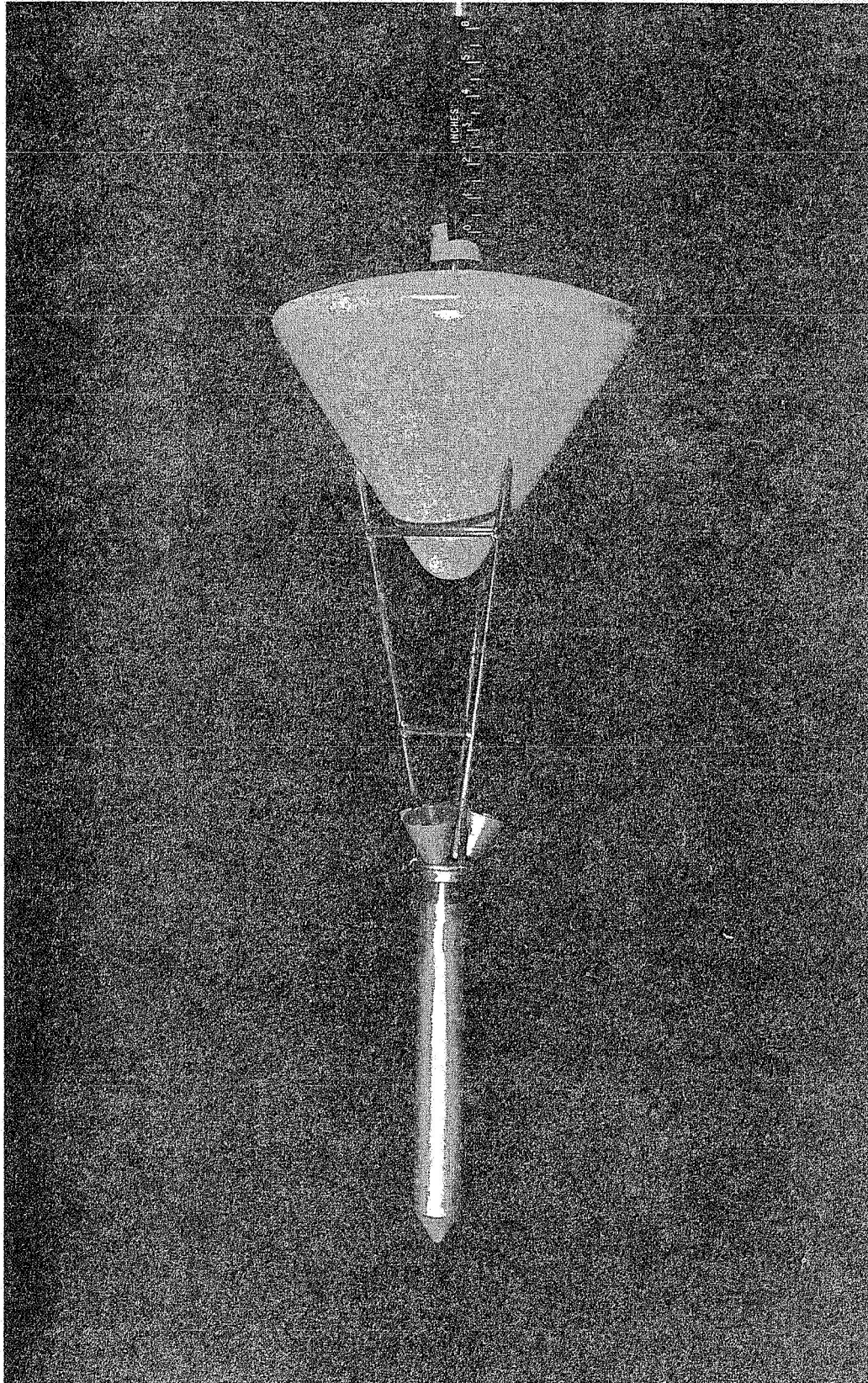Figure 2d. - Solid abort tower configuration.

D=10.92

29.71

11.4

8.29

−0.04070

.706 D

A—A

B—B

Section B-B

5.3

Section A-A

8.3

Sketch of ring device showing
general dimensions.

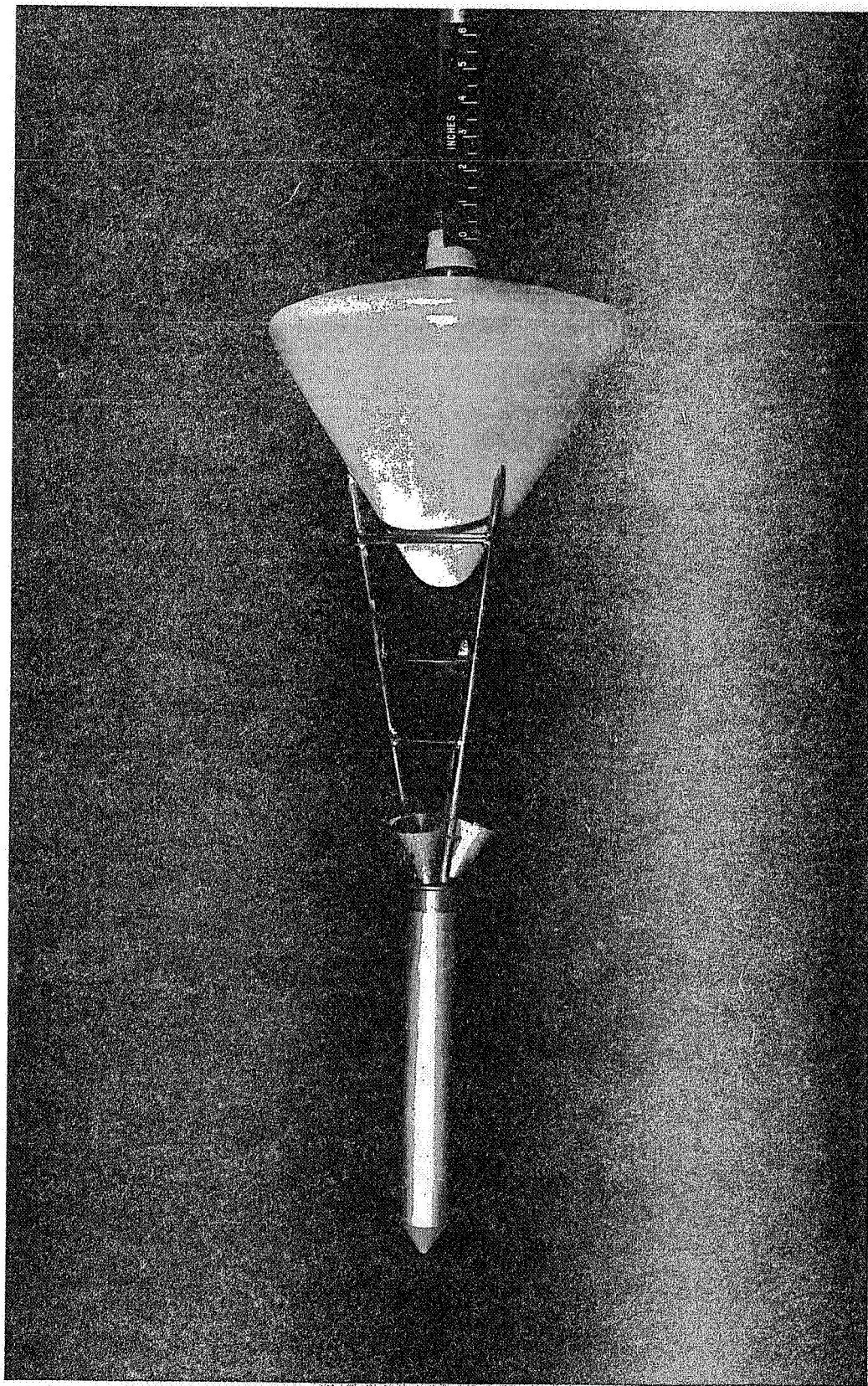Figure 2e. - Abort configuration with flow deceleration ring device.

(a) Atmospheric abort configuration will have turning vane mounted at the base of the rocket.

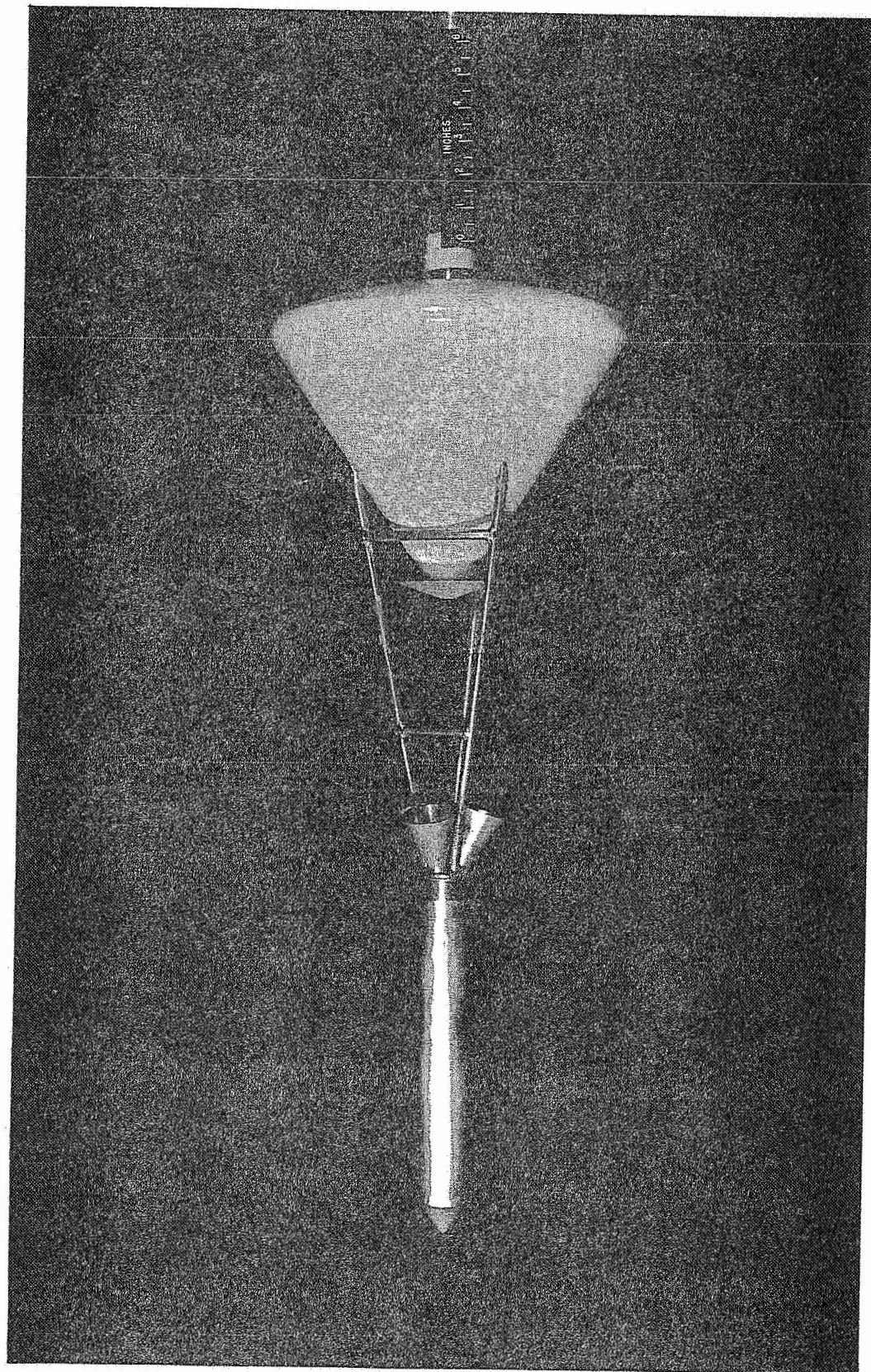Figure 3.- Photographs of the configurations tested.

(b) Atmospheric abort configuration with small turning vane mounted at the base of the rocket case.
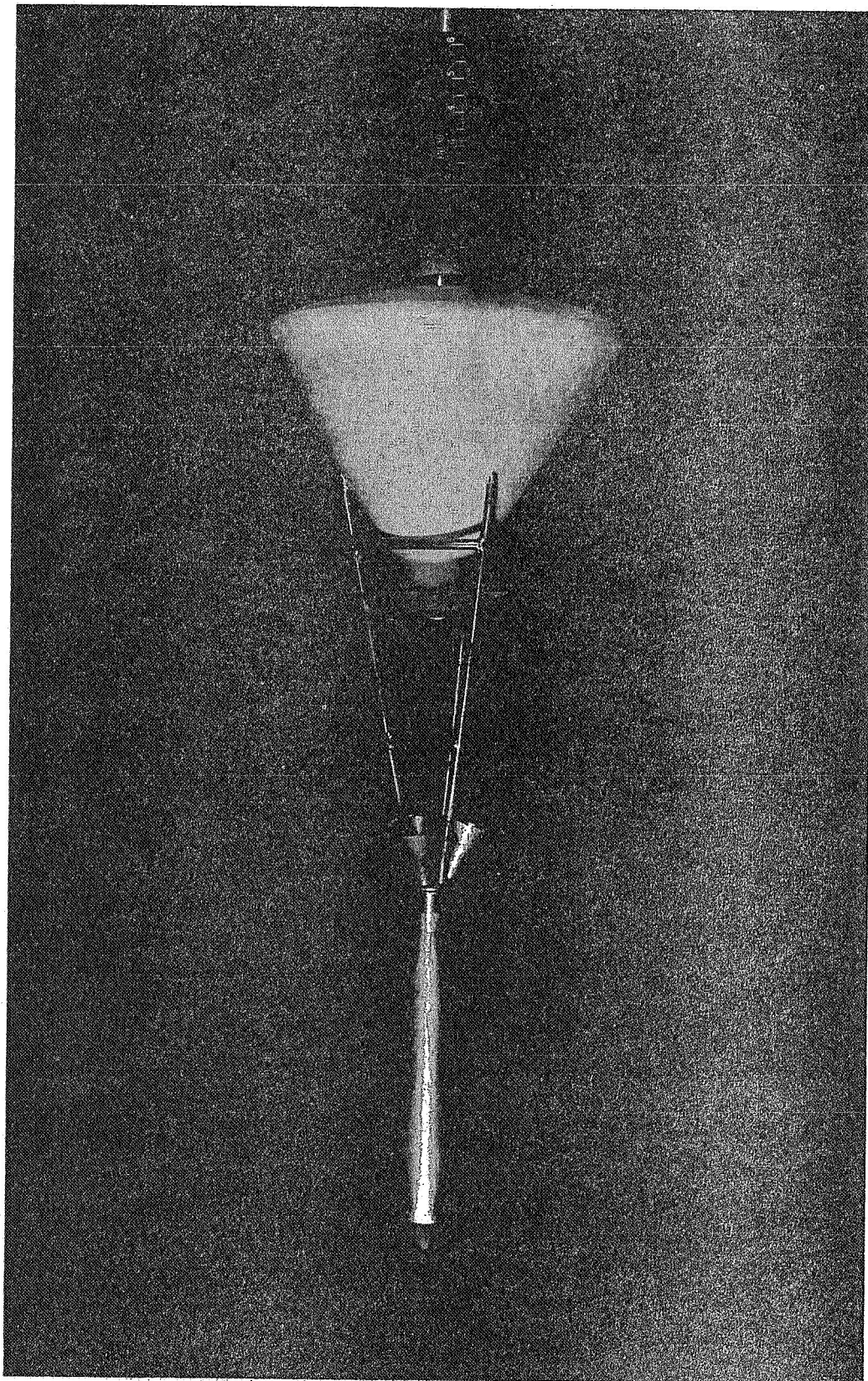
Figure 3.- Continued.

(c) Atmospheric abort configuration with blunt-cone shield mount within the abort tower near the tower midpoint.
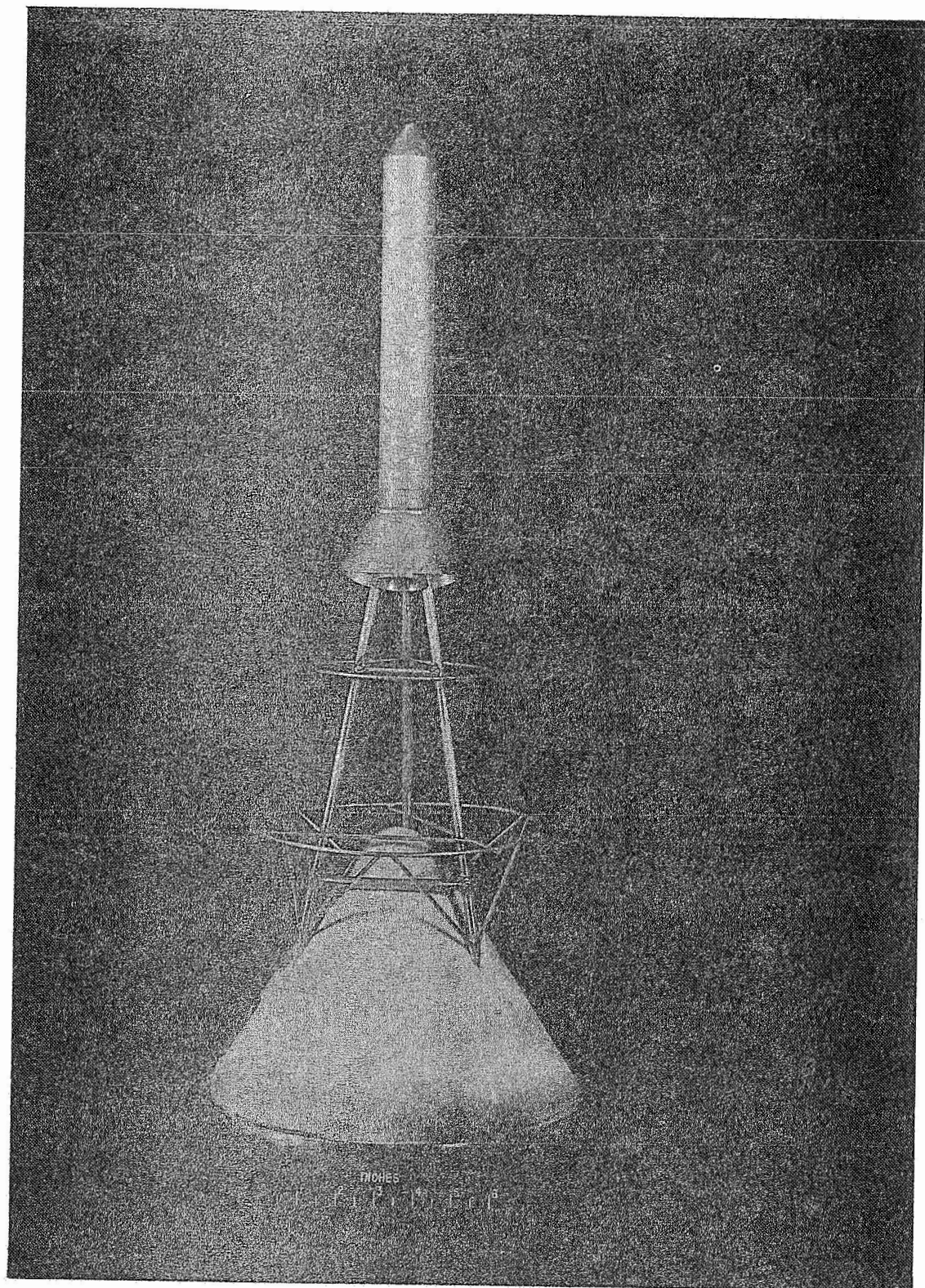
Figure 3.- Continued.

(d) Atmospheric abort configuration with small blunt-cone shield mounted at spacecraft nose.
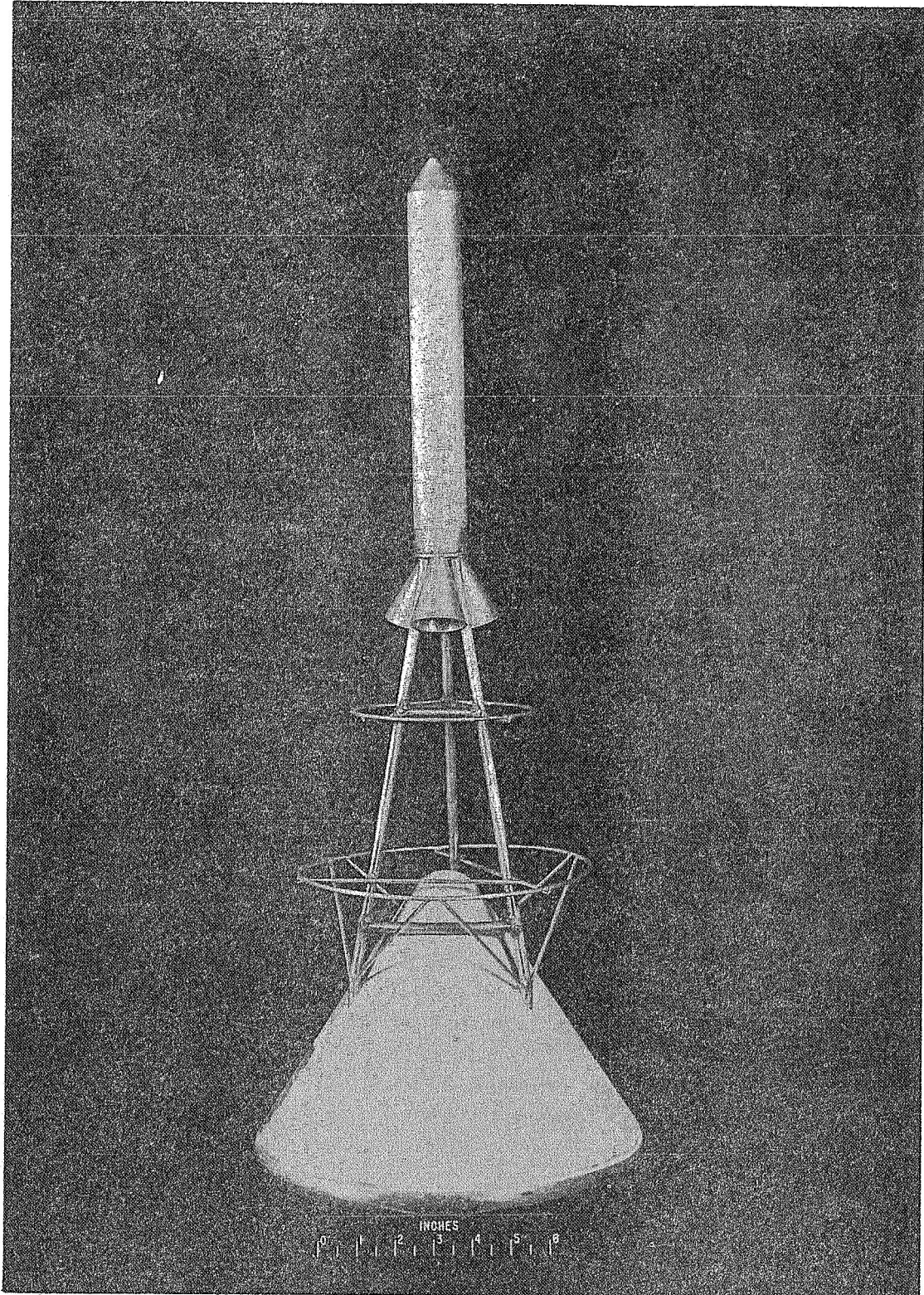
Figure 3.- Continued.

(e) Atmospheric abort configuration with large blunt-cone shield mounted at spacecraft nose.

Figure 3.- Continued.

(f) Atmospheric abort configuration with a flow
decoleration ring device with the conical
shroud.
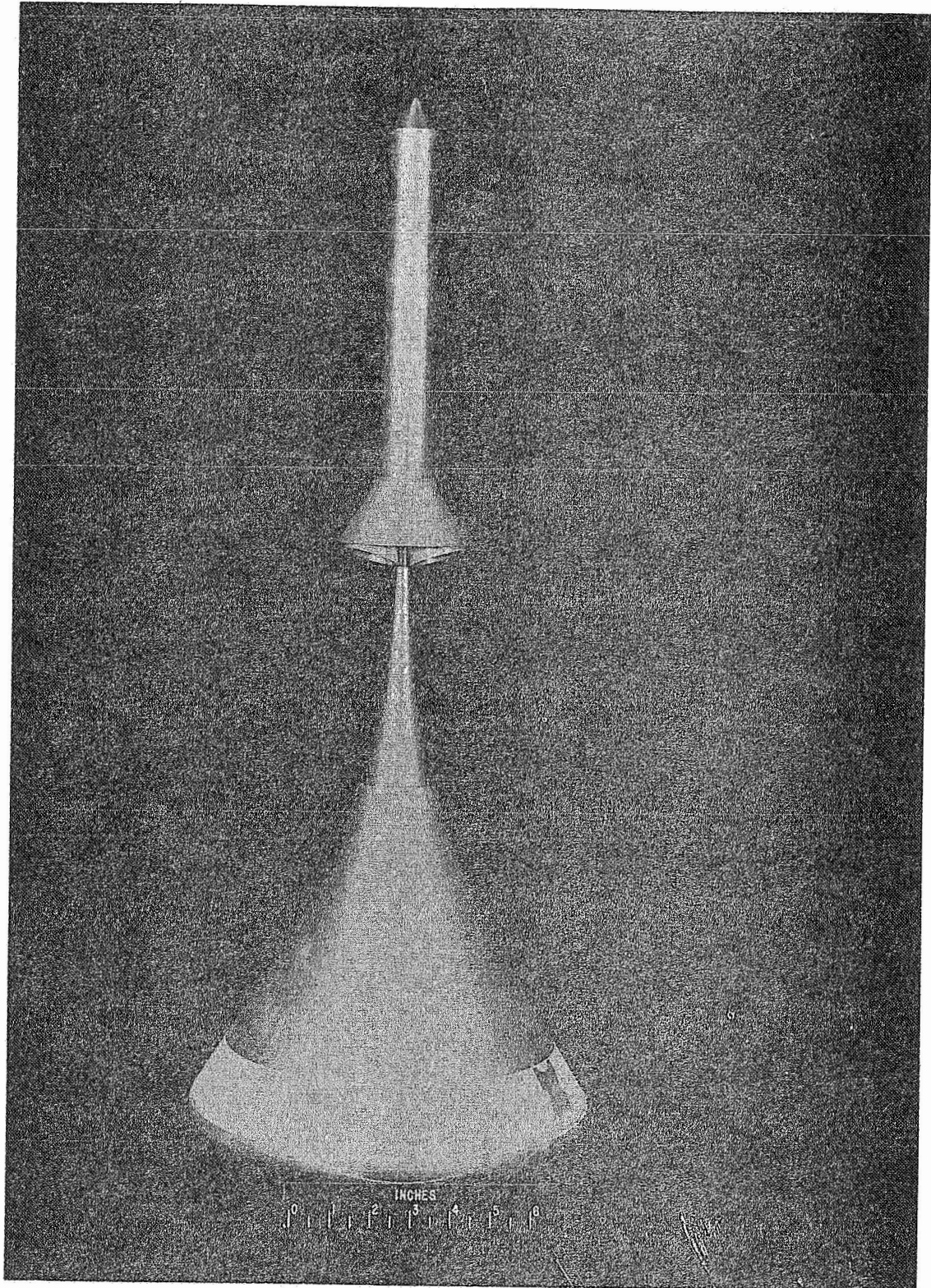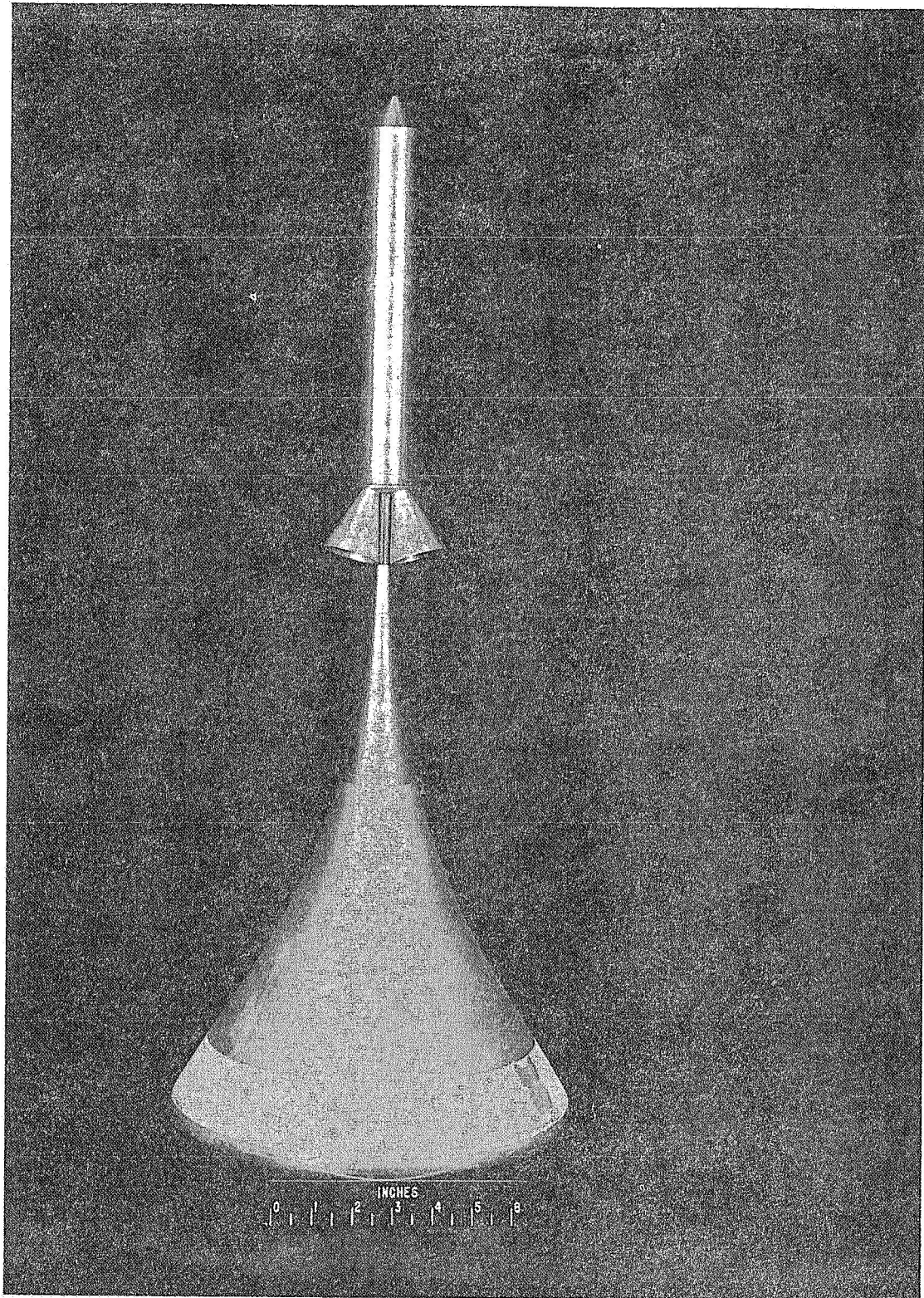
Figure 3.- Continued.

(g) Atmospheric abort configuration with a flow
     deceleration ring device without the conical
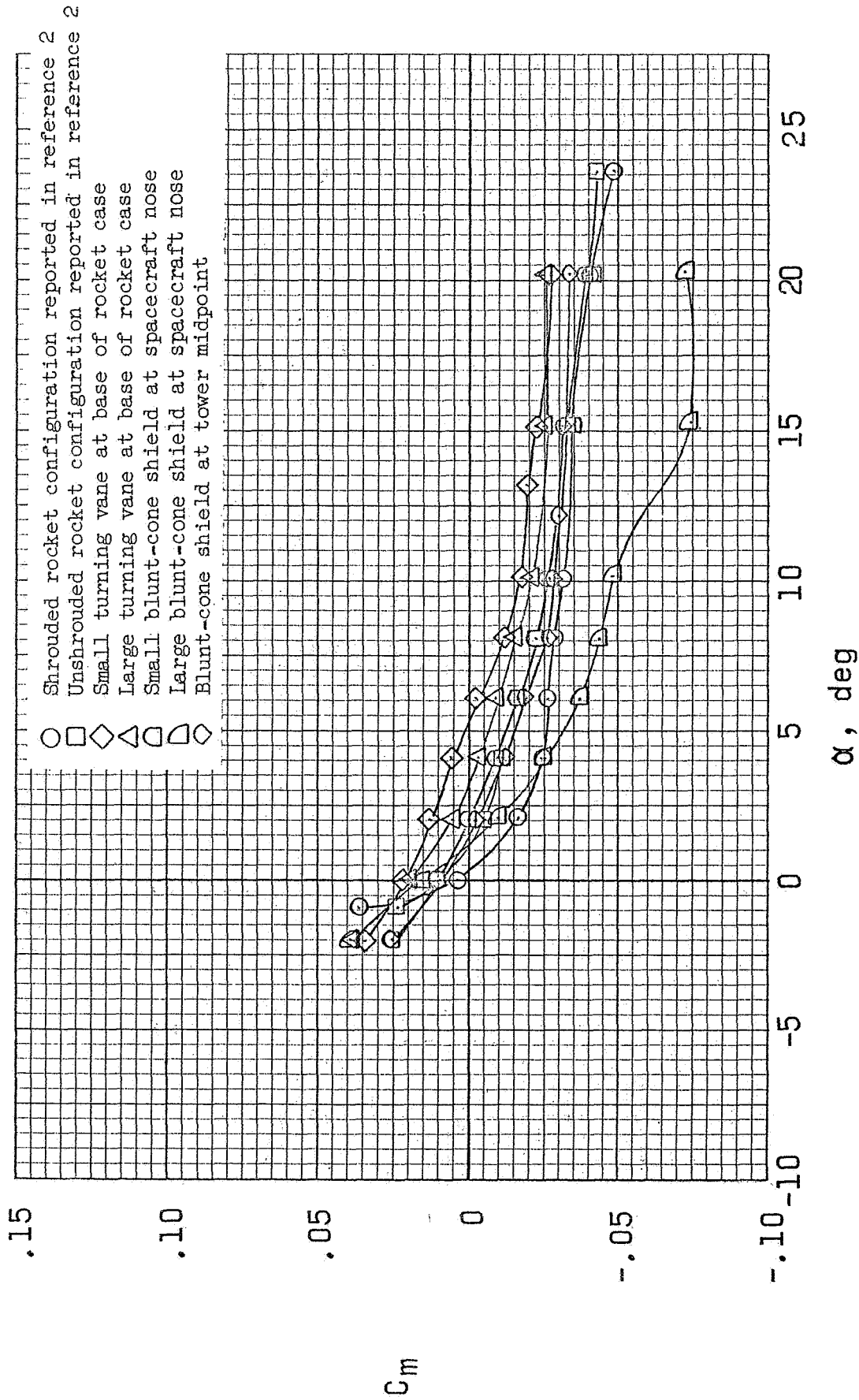   shroud.

Figure 3.- Continued.

(h) Solid abort tower configuration with the
conical shroud.

Figure 3.- Continued.

24

(i) Solid abort tower configuration without the
conical shroud.

Figure 3.- Concluded.

Symbols (legend):

○ Shrouded rocket configuration reported in reference 2
□ Unshrouded rocket configuration reported in reference 2
◇ Small turning vane at base of rocket case
◁ Large turning vane at base of rocket case
⬠ Small blunt-cone shield at spacecraft nose
⬠ Large blunt-cone shield at spacecraft nose
◇ Blunt-cone shield at tower midpoint

α, deg

C_m

(a) Pitching-moment coefficient. M = 0.5.

Figure 4.- Transonic static stability characteristics of several modifications to the atmospheric abort configuration reported in reference 2.

Shrouded rocket configuration reported in reference 2
Unshrouded rocket configuration reported in reference 2
Small turning vane at base of rocket case
Large turning vane at base of rocket case
Small blunt-cone shield at spacecraft nose
Large blunt-cone shield at spacecraft nose
Blunt-cone shield at tower midpoint
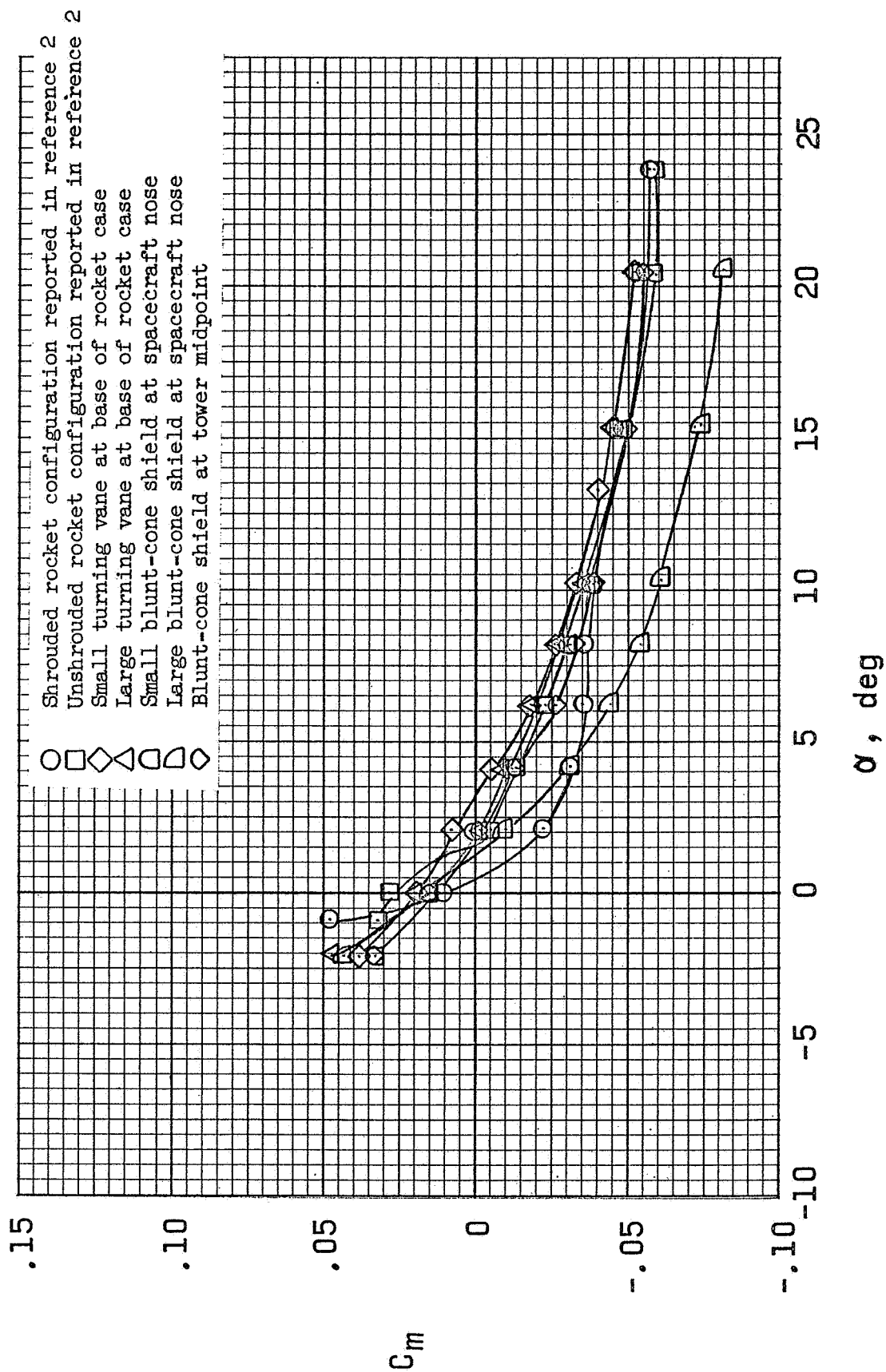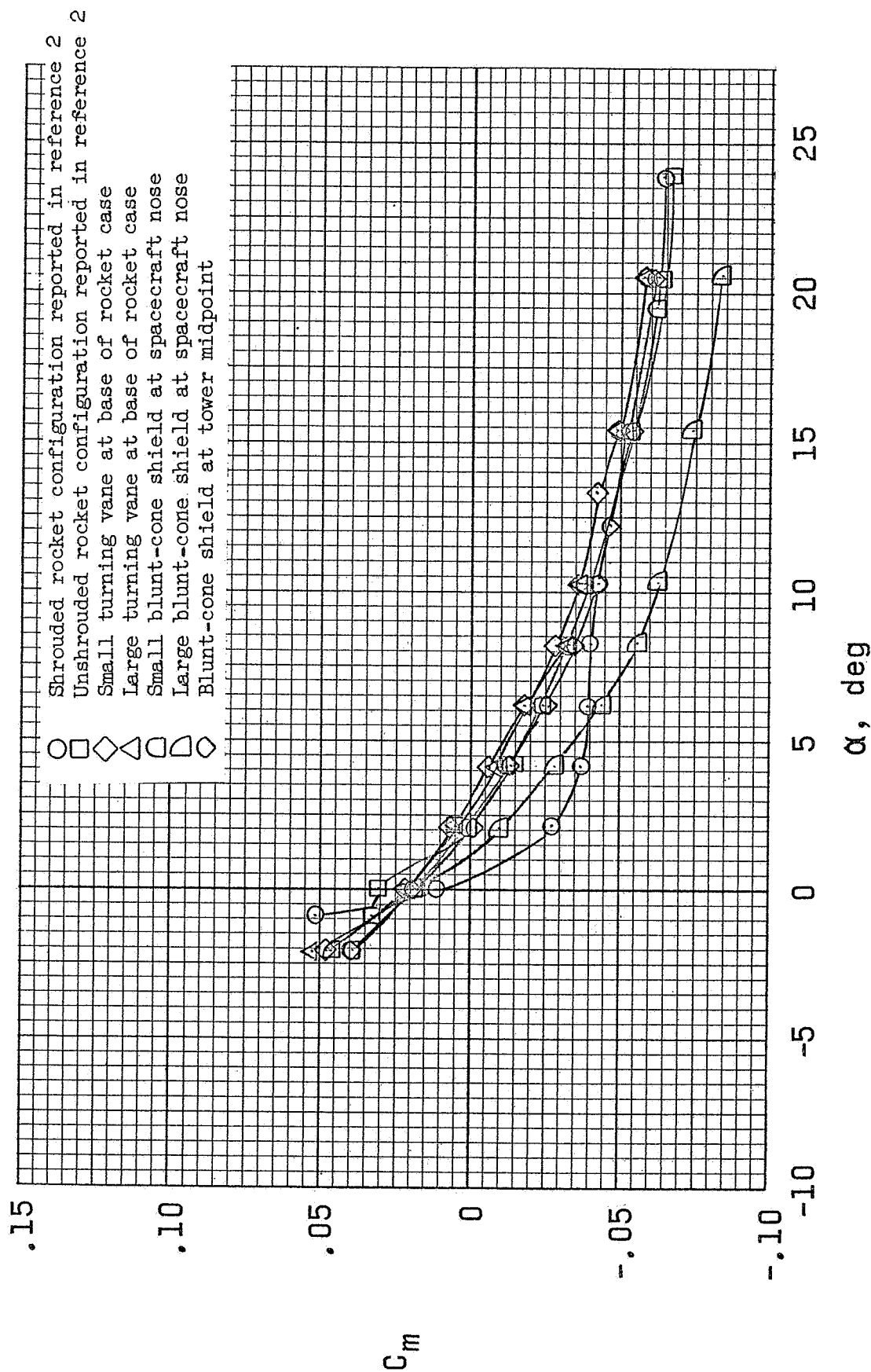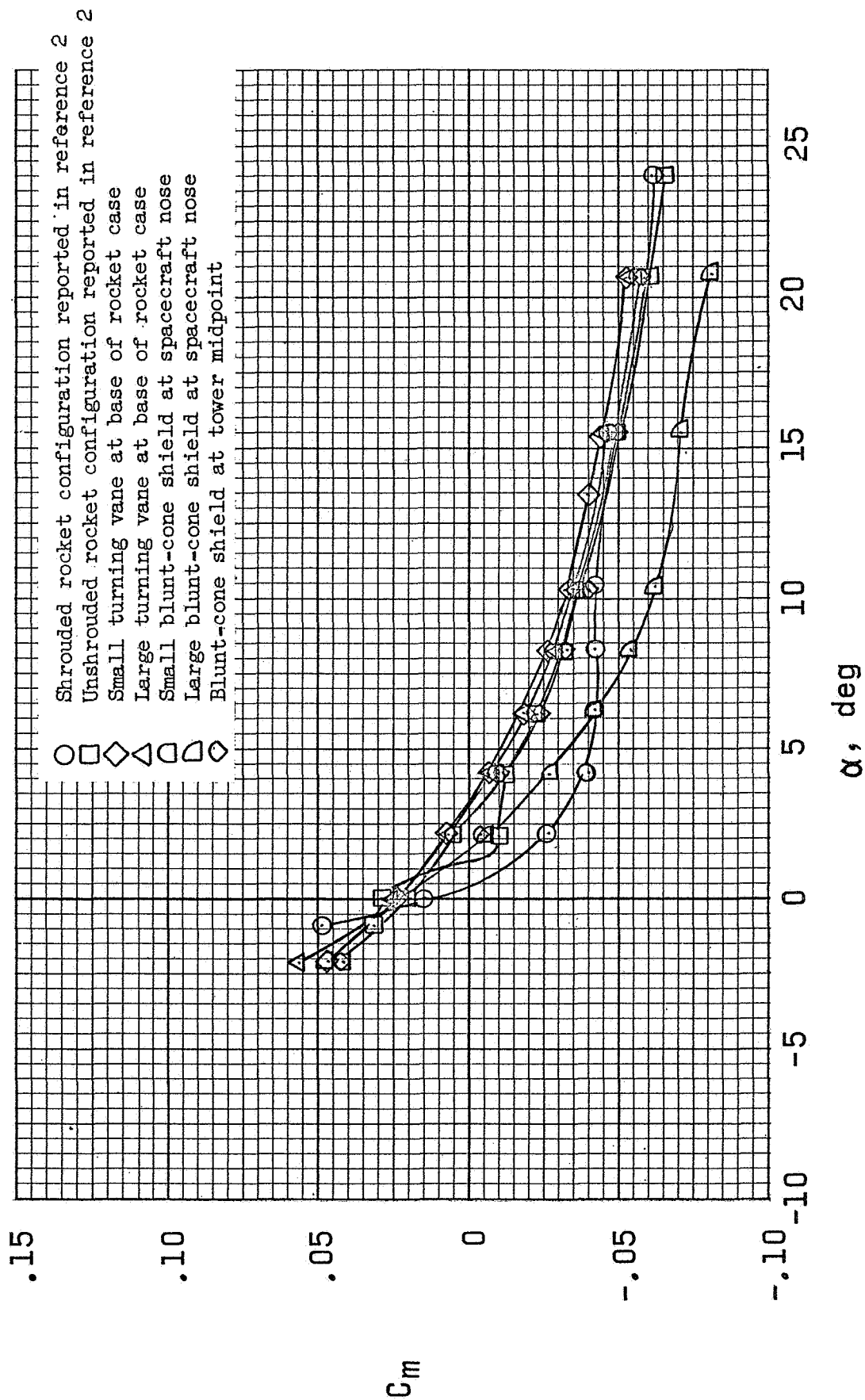
(b) Pitching-moment coefficient. M = 0.7.

Figure 4. - Continued.

(c) Pitching-moment coefficient. M = 0.8.

Figure 4. - Continued.

O Shrouded rocket configuration reported in reference 2
□ Unshrouded rocket configuration reported in reference 2
◇ Small turning vane at base of rocket case
◁ Large turning vane at base of rocket case
◻ Small blunt-cone shield at spacecraft nose
◹ Large blunt-cone shield at spacecraft nose
◇ Blunt-cone shield at tower midpoint

(d) Pitching-moment coefficient. M = 0.9

Figure 4.- Continued.

Shrouded rocket configuration reported in reference 2
Unshrouded rocket configuration reported in reference 2
Small turning vane at base of rocket case
Large turning vane at base of rocket case
Small blunt-cone shield at spacecraft nose
Large blunt-cone shield at spacecraft nose
Blunt-cone shield at tower midpoint
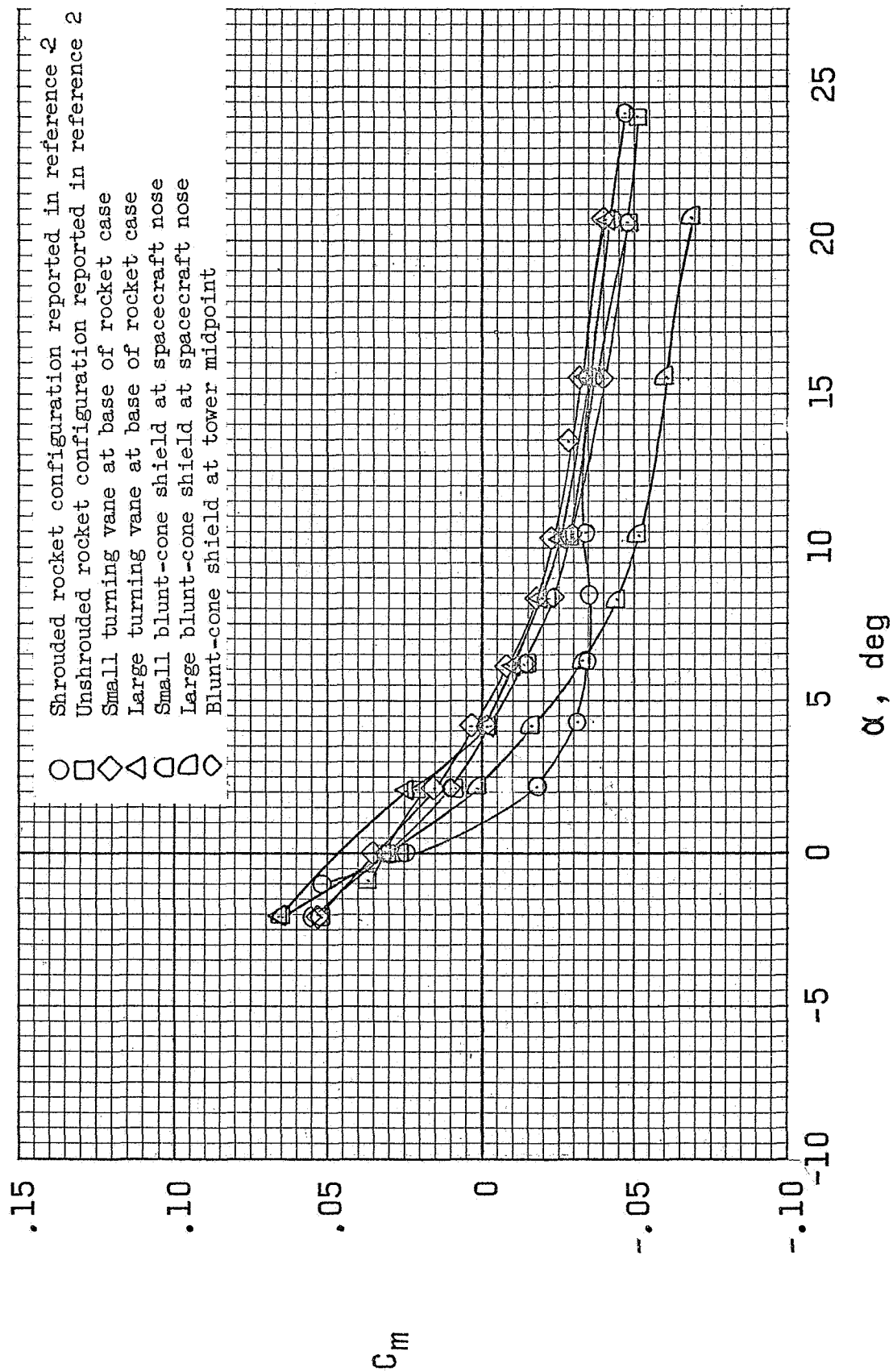
(e) Pitching-moment coefficient, M = 1.00

Figure 4. - Continued.

30

Legend:
○ Shrouded rocket configuration reported in reference 2
□ Unshrouded rocket configuration reported in reference 2
◇ Small turning vane at base of rocket case
◁ Large turning vane at base of rocket case
⬠ Small blunt-cone shield at spacecraft nose
⬡ Large blunt-cone shield at spacecraft nose
◇ Blunt-cone shield at tower midpoint
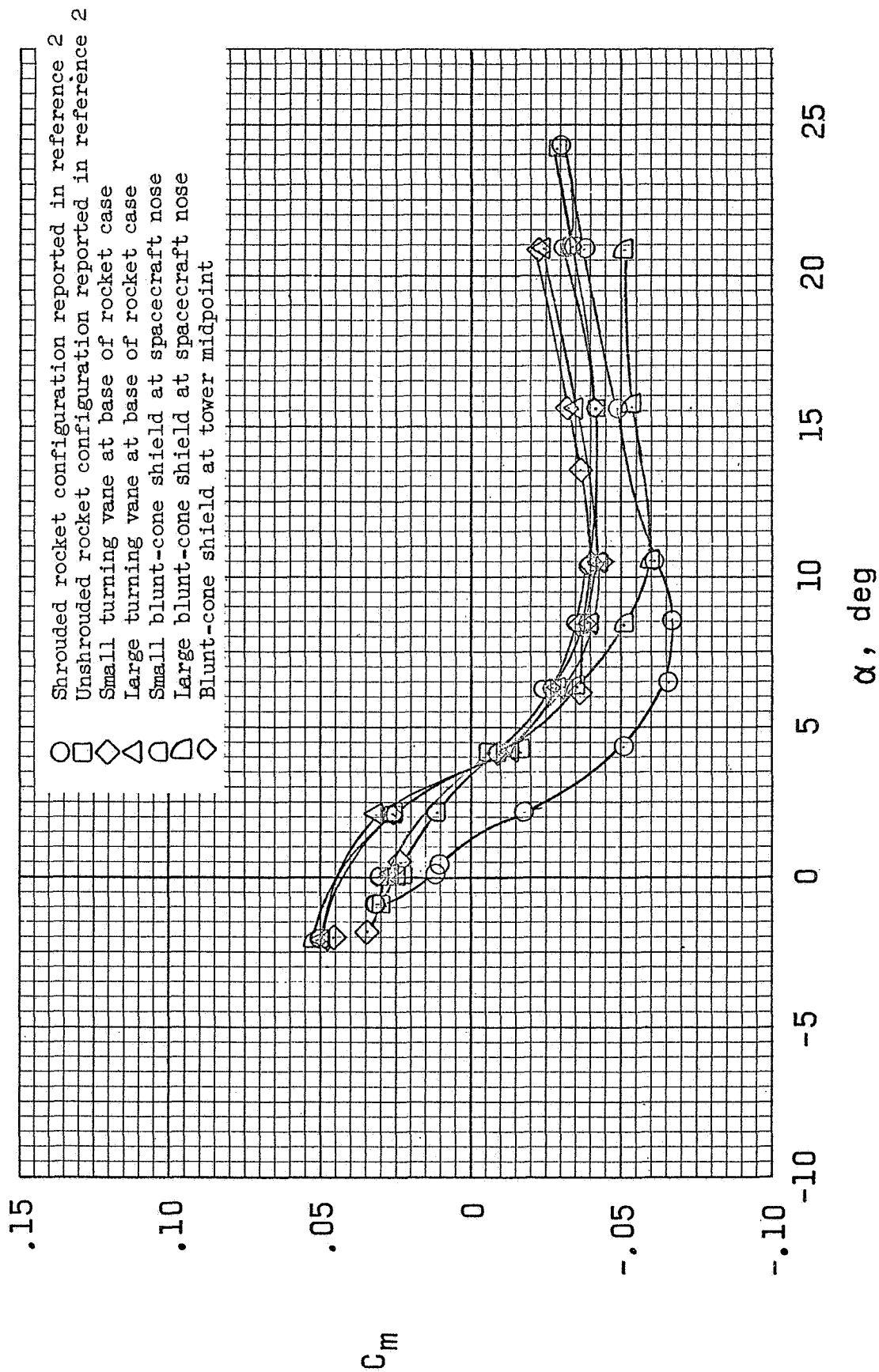
(f) Pitching-moment coefficient. M = 1.20.

Figure 4. - Concluded.

(a) Pitching-moment coefficient. M = 1.57.

Figure 5.- Supersonic static stability characteristics of
a solid abort tower configuration and one modification
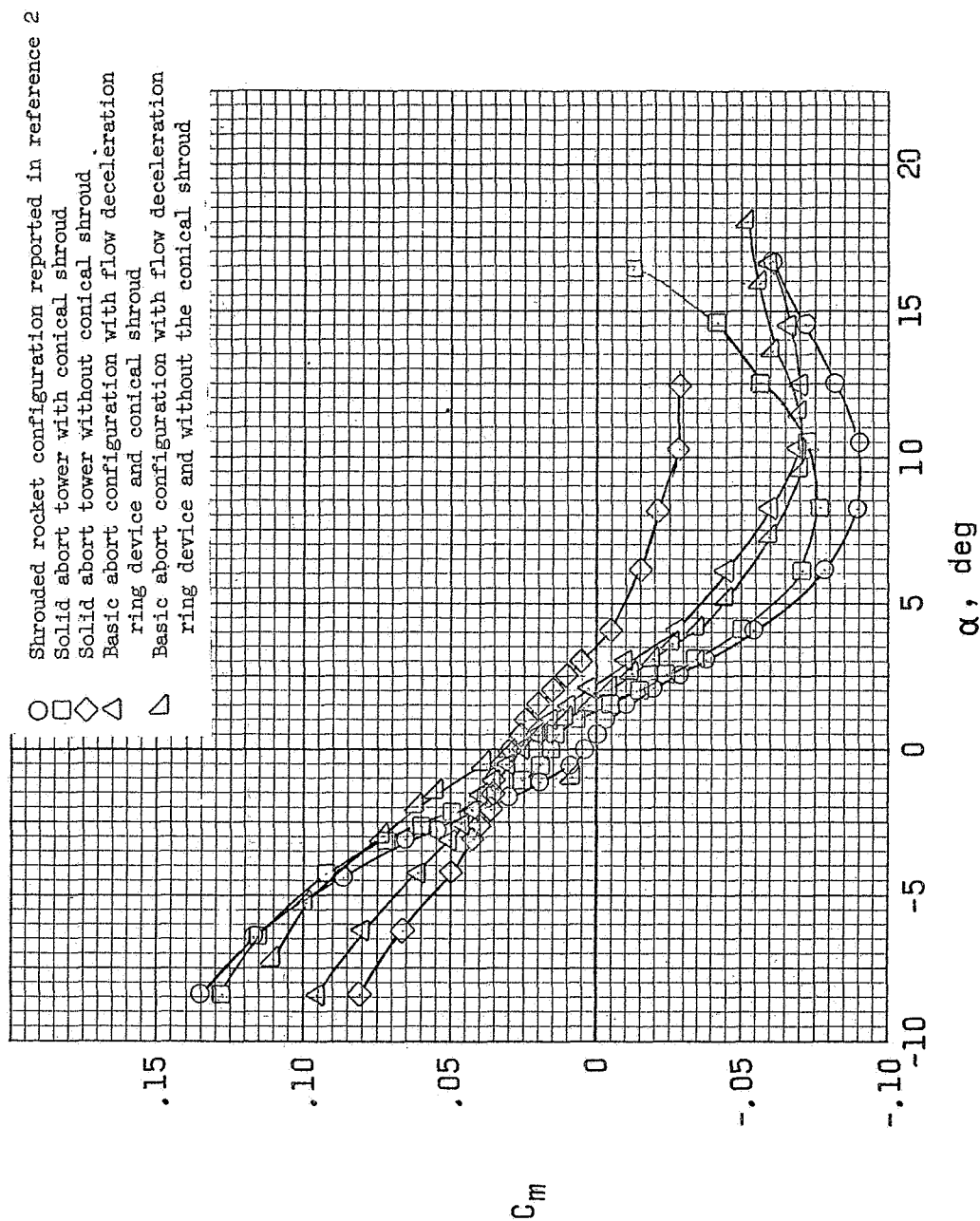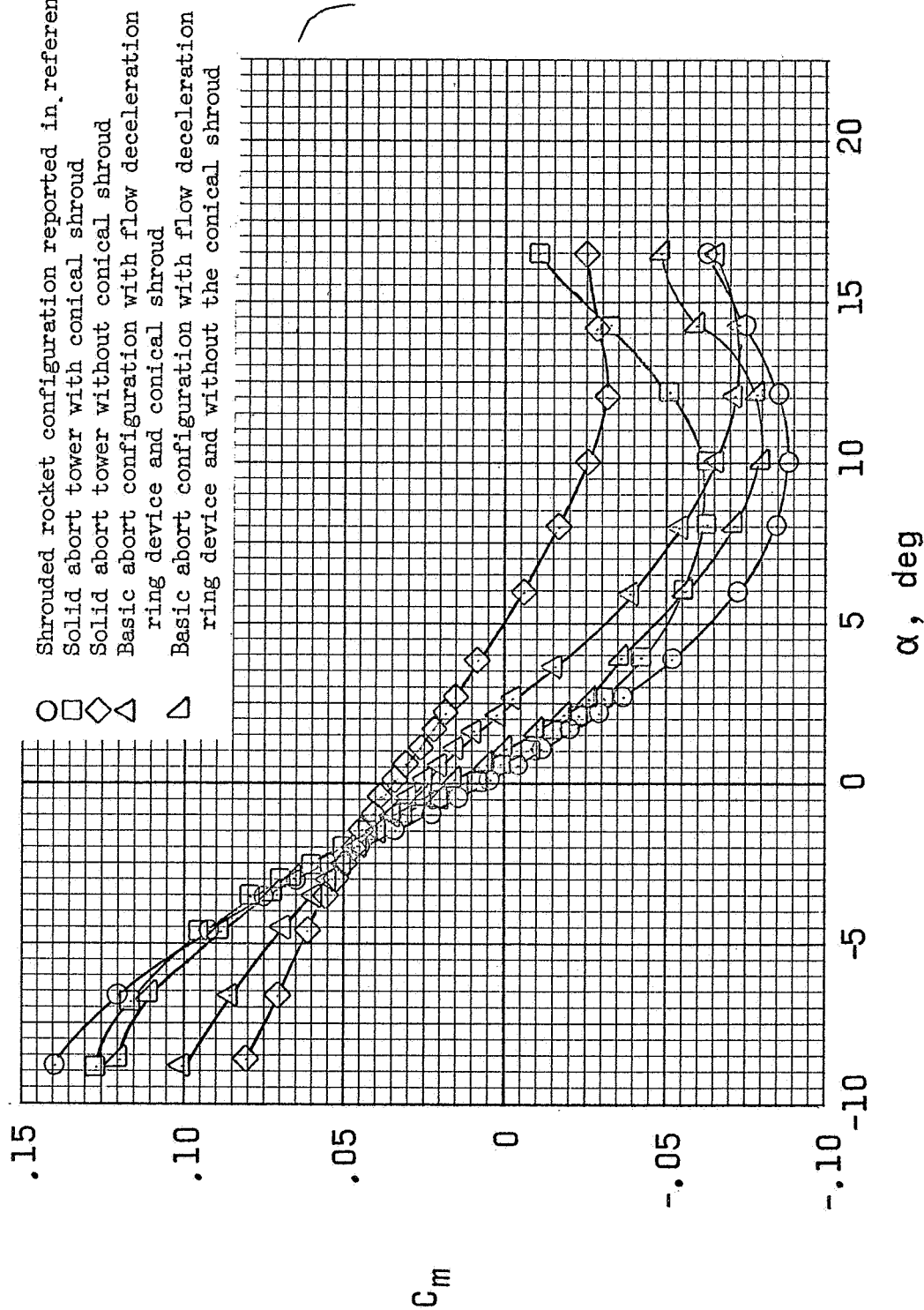to the atmospheric abort configuration reported in
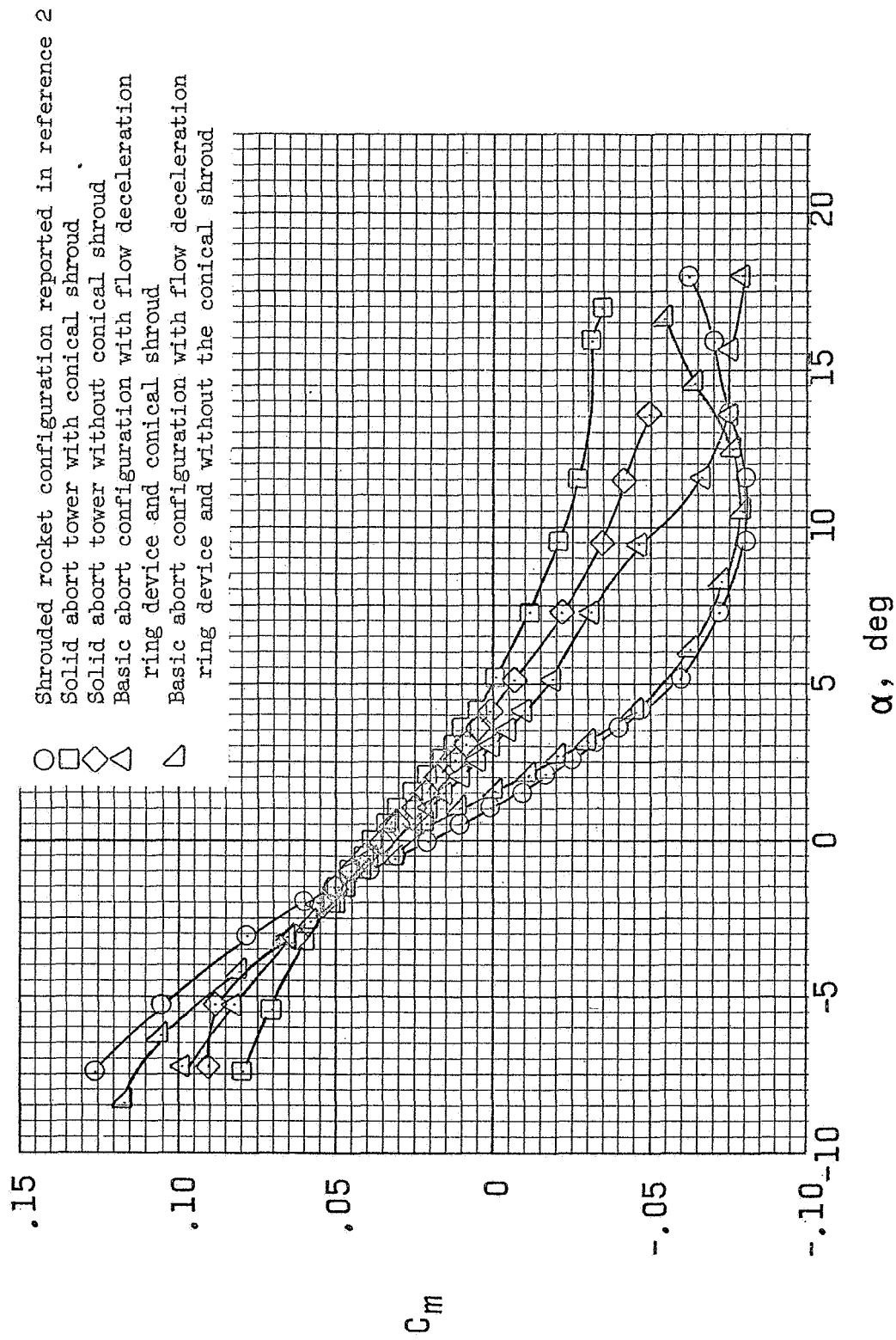reference 2.

(b) Pitching-moment coefficient. M = 1.80.

Figure 5. - Continued.

(c) Pitching-moment coefficient. M = 2.16.

Figure 5.- Concluded.

Distribution - Apollo Working Paper No. 1044

Copy   Addressees

1   Director
2   Associate Director
3-8   Technical Information Library (6)
9   Asst Director for Research and Development
10-12   Project Offices (3)
13   Reliability and Flight Safety Office
14   Public Affairs Office
15-16   NASA Headquarters, Attn: Mr. G. M. Low, MS (2).
17   Spacecraft Research Division
18   Flight Dynamics Branch
19   Aerodynamics Section
20-29   Technical Information Division Storage (10)